

# Design and Analysis Of DC-AC Soft Switching Converter

*A Project report submitted in partial fulfilment  
of the requirements for the degree of B. Tech in Electrical Engineering*

*By*

**BITAN SARKAR (11701618054)  
KOMAL KUMARI (11701618041)  
ARANNYA MANDOL (11701618057)  
SOURO KISHORE BHATTACHARYA (11701619051)**

*Under the supervision of*

**Mr. Sarbojit Mukherjee  
Assistant Professor, Dept. of EE  
RCCIIT**



*Department of Electrical Engineering*

**RCC INSTITUTE OF INFORMATION TECHNOLOGY**

CANAL SOUTH ROAD, BELIAGHATA, KOLKATA – 700015, WEST BENGAL

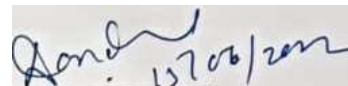
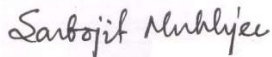
Maulana Abul Kalam Azad University of Technology (MAKAUT)

© 2022

## ***CERTIFICATE***

### **To whom it may concern**

This is to certify that the project work entitled **Design and Analysis Of DC-AC Soft Switching Converter** is the bona fide work carried out by **BITAN SARKAR (11701618054), KOMAL KUMARI (11701618041), ARANNYA MANDOL (11701618057), SOURO KISHORE BHATTACHARYA (11701619051)** , the students of B.Tech in the Dept. of Electrical Engineering, RCC Institute of Information Technology (RCCIIT), Canal South Road, Beliaghata, Kolkata-700015, affiliated to Maulana Abul Kalam Azad University of Technology (MAKAUT), West Bengal, India, during the academic year 2021-22, in partial fulfillment of the requirements for the degree of Bachelor of Technology in Electrical Engineering and this project has not submitted previously for the award of any other degree, diploma and fellowship.



\_\_\_\_\_  
**Signature of the Guide**

\_\_\_\_\_  
**Signature of the HOD, EE**

**Name: Mr. Sarbojit Mukherjee**

**Name: Prof. Dr. Debasish Mandol**

**Designation: Asst. Prof. Dept. of EE,**

**Designation: HOD, Electrical Dept.,**

**RCCIIT**

**RCC Institute of Information Technology**



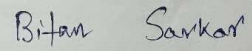
\_\_\_\_\_  
**Signature of the External Examiner**

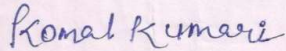
## ***ACKNOWLEDGEMENT***

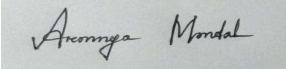
It is my great fortune that I have got opportunity to carry out this project work under the supervision of **Mr. Sarbojit Mukherjee** in the Department of Electrical Engineering, RCC Institute of Information Technology (RCCIIT), Canal South Road, Beliaghata, Kolkata -700015, affiliated to Maulana Abul Kalam Azad University of Technology (MAKAUT), West Bengal, India. I express my sincere thanks and deepest sense of gratitude to my guide for his constant support, unparalleled guidance and limitless encouragement.

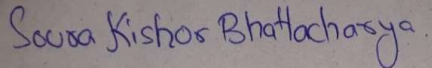
I wish to convey my gratitude to Prof. (Dr.) Debasish Mondal, HOD, Department of Electrical Engineering, RCCIIT and to the authority of RCCIIT for providing all kinds of infrastructural facility towards the research work.

I would also like to convey my gratitude to all the faculty members and staffs of the Department of Electrical Engineering, RCCIIT for their whole hearted cooperation to make this work turn into reality.

**BITAN SARKAR (11701618054)** 

**KOMAL KUMARI (11701618041)** 

**ARANNYA MANDOL (11701618057)** 

**SOURO KISHORE BHATTACHARYA (11701619051)** 

-----  
**Signature of the Students**

## **Table of Contents**

<b>Topic</b>	<b>Page No.</b>
1. List of Acronyms	7
2. Introduction and Theory	8
2.1. Bidirectional DC-DC Converter	10
2.1.1. Non-isolated Bidirectional Converter	10
2.1.2. Isolated Bidirectional Converter	11
2.2. Necessity of Isolation	12
2.3. Types of Isolation	13
2.3.1. Transformer	13
2.3.2. Relay	14
2.3.3. Hall Effect Sensor	15
2.4. Applications of galvanic Isolation	16
2.5. Types of DC-DC Converter	17
2.5.1. Linear Mode	17
2.5.2. Hard Switching Mode	17
2.5.3. Soft Switching Mode	18
2.6. Necessity of Soft Switching technique	18
2.7. Merits and demerits of DC-DC Converter	19
2.8. Resonant converter	20
2.8.1. ZVS Mode	21
2.8.2. ZCS Mode	22
3. Literature Review	24
3.1. Converter with HVDC & LVDC Application	25
3.2. Converter with DAB and MEA topology	27
3.3. Converter with Current Doubler topology	29
3.4. Super-lift LUO Converter in EV applications	29
3.5. SPWM inverter for Digitized Signal generation	30
3.6. SPWM for Carrier frequency modulation	31
3.7. Multi-level Inverter with SPWM Control	33
3.8. DC-DC Converter with application based topologies	33

4. Working Principle	35
4.1. DC-DC Converter	36
4.1.1. Buck Mode	36
4.2.2. Boost Mode	39
4.2. SPWM Inverter	42
5. Circuit Diagram	46
5.1. DC-DC Bidirectional Converter	47
5.2. Three Phase Inverter	47
6. Mathematical Modelling	48
6.1. DC-DC Converter	49
6.1.1. Boost Mode	49
6.1.2. Buck Mode	51
6.2. DC-AC Converter	51
7. Software Simulation	54
7.1. Overall Block Diagram	55
7.2. DC-DC Buck-Boost bidirectional converter	55
7.2.1. Boost Mode	55
7.2.2. Buck Mode	56
7.3. DC-AC Converter (Inverter)	56
7.4. Load	57
7.5. SPWM Pulse Generation Circuit	57
8. Observation and Results	58
8.1. Battery parameters	59
8.1.1. Boost Mode	59
8.1.2. Buck Mode	59
8.2. Boost Mode Switching and Inductor parameters	60
8.3. Buck Mode Switching and Inductor parameters	61
8.4. Transformer Parameters	62
8.4.1. Boost Mode	62
8.4.2. Buck Mode	62
8.5. Graph of Inverter Output at Resistive Load	63
8.5.1. Buck Mode	63

8.5.2. Boost Mode	63
8.6. Load Curve	64
8.6.1. Buck Mode	64
8.6.2. Boost Mode	64
8.7. SPWM Pulse generation Curve	65
8.8. Outcome Values of each parameter	65
8.8.1. Boost Mode	65
8.8.2. Buck Mode	66
9. Conclusion	67
10. APENDIX	
A. Specifications and Standard Values	69
B. References	71

## **List of Acronyms**

1. IBDC – Isolated Bidirectional DC-DC Converter
2. NBDC – Non-Isolated Bidirectional DC-DC Converter
3. MOSFET – Metal Oxide Semiconductor Field Effect Transistor
4. IGBT – Insulated Gate Bipolar Transistor
5. UPS – Uninterrupted Power Supply
6. SMPS – Switching Mode Power Supply
7. EMI – Electromagnetic Interference
8. ZVS – Zero Voltage Switching
9. ZCS – Zero Current Switching
10. PWM – Pulse Width Modulation
11. SPWM – Sinusoidal Pulse Width Modulation
12. PFC – Power Factor Correction
13. FACTS – Flexible Alternating Current Transmission System
14. GSSA – Generalized State Space Averaging
15. ESS – Electrical Storage System
16. AEA – Antenna Electronics Assembly
17. MEA – More Electronic Assembly
18. HVDC – High Voltage direct Current
19. LVDC – Low Voltage Direct Current
20. DAB – Dual Active Bridge
21. TT – Triangular Trapezoidal modulation
22. MIL -STD – Military Standard
23. CD – Current Doubler
24. WBG – Wide band Gap
25. ABAC – Active Bridge Active clamp
26. MPC – Multi-port Converter
27. HEV – Hybrid Electrical Vehicle
28. PV – Photo-Voltaic system
29. GaN – Gallium Nitride
30. SiC – Silicon Carbide
31. SIDO – Single Input Dual output
32. SIMO – Serial Input Multi-Output
33. SLBC – Super Lift and Buck Converter
34. FPLD – Field Programmable Logic Device
35. FPGA – Field Programmable Gate Array
36. CFM – Carrier Frequency Modulation
37. MCFT – Modulating Carrier Frequency Twice
38. DSP – Digital Signal Processing
39. USB – Universal Serial Bus
40. CPU – Central Processing Unit
41. DRAM – Dynamic Random Access Memory

# Chapter 1

## (Introduction & Theory)

- Introduction



For the electrical power sources like Photovoltaic cells, Batteries, utility supplies (like UPS), the conventional loads are not compatible with direct connections because of some practical limitations related to *ratings of passive components, current tolerance and voltage withstanding capability*. That's why, to make them capable with the above mentioned power sources, a specific type of interfacing arrangements have to be added in between the source side and the receiving side (in case of any emergency, opposite direction power flow is also needed) so that currents, voltage and other necessary parameters are accordingly scaled and manipulated. For this purpose, **DC-AC** and **DC-DC** Converter (generally known as **Inverter** and **Chopper** respectively) is popularly and conventionally used.

With the rapid development of modern energy applications such as renewable energy, *PV* systems, electric vehicles, and smart grids, *DC-DC* converters have become the fundamental component to meet the proper industrial requirements. Advanced converters are effective in reducing switching losses and providing an efficient energy conversion. Yet the key challenge is to provide a single converter that has all the desired and required features to deliver efficient energy for various types of modern energy systems and energy storage system integrations. Here a small review is given on ***multilevel, bidirectional, and resonant converters*** w.r.t. their architecture, classifications, positive and negative sides, combined topologies, applications, and challenges; practical recommendations were also made to provide clear cut ideas of the recent challenges and bounded capabilities of these three converters to guide the engineering as well as common society on improving and providing a new, economically and functionally efficient converter that meets the strict demands of modern energy system integrations. The needs of other industrial applications as well as the number of elements under usage for lowering the size and weight, were also considered to achieve a power circuit that can efficiently mitigate the limitations under concern. Shortly we can say that, integrated bidirectional resonant *DC-DC* converters and multilevel inverters are expected to be well suited and are in rising demand for several applications in the near future.

### ➤ **Bidirectional Converter**

Basic dc-dc converters such as buck and boost converters (and their derivatives) do not have bidirectional power flow capability. This limitation is due to the presence of diodes in their structure which prevents reverse current flow. In general, a unidirectional dc-dc converter can be turned into a bidirectional converter by replacing the diodes with a controllable switch in its structure. The bidirectional dc-dc converter along with energy storage has become a promising option for many power related systems, including hybrid vehicle, fuel cell vehicle, renewable energy system and so forth. It not only reduces the cost and improves efficiency, but also improves the performance of the system. Basically the bidirectional converters are divided into two types, non-isolated and isolated converters, meeting different application requirements.

Most of the existing bidirectional dc-dc converters fall into the generic circuit structure illustrated in Figure, which is characterized by a current fed or voltage fed on one side. Based on the placement of the auxiliary energy storage, the bidirectional dc-dc converter can be categorized into buck and boost type. The buck type is to have energy storage placed on the high voltage side, and the boost type is to have it placed on the low voltage side. To realize the double sided power flow in bi-directional dc-dc converters, the switch cell should carry the current on both directions. It is usually implemented with a unidirectional semiconductor power switch such as power MOSFET (Metal-Oxide-Semiconductor-Field-Effect-Transistor) or IGBT (Insulated Gate Bipolar Transistor) in parallel with a diode; because the double sided current flow power switch is not available. For the buck and boost dc-dc type converters, the bidirectional power flow is realized by replacing the switch and diode with the double-sided current switch cell.

#### ***A. Non-isolated Bidirectional DC-DC Converters***

In the transformer-less non-isolated power conversion systems, the boost type and buck type dc-dc converter are chosen usually. The high frequency transformer based system is an attractive one to obtain isolation between the source and load sides. But from the view point of improving the efficiency, size, weight and cost, the transformer-less type is much more attractive. Thus, in the high power or spacecraft power system applications, where weight or

size is the main concern, the transformer-less type is more attractive in high power applications. Non-isolated BDCs (NBDC) are simpler than isolated BDCs (IBDC) and can achieve better efficiency the transformer-less type is more attractive in high power applications. For the present high power density bidirectional dc-dc converter, to increase its power density, multiphase current interleaving technology with minimized inductance has been found in high power applications. The operation of the NBDC of Fig. as follows. The inductor is the main energy transfer element in this converter. In each switching cycle it is charged through source side active switch for the duration of  $T_{on}=DT$ , where  $T=1/f_{sw}$  is the switching period and  $D$  is the duty cycle. This energy is then discharged to load during  $T_{off}=(1-D)T$ .

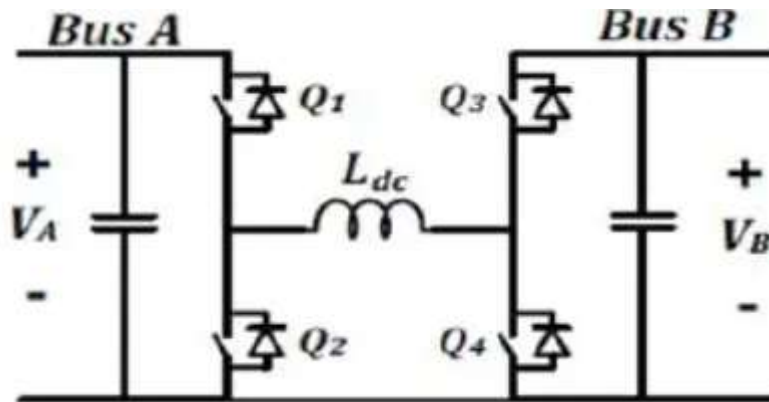


*Fig: 1- two back-to-back connected non-isolated bidirectional DC-DC Converter*

In the four-switch buck boost converter the principle of operation is the same. In the left to right power transfer mode,  $Q_1$  and  $Q_4$  act as active switches, while in the right to left power transfer the opposite switches ( $Q_2$  and  $Q_3$ ) are controlled. Synchronous rectification technique can be employed in this configuration in order to add more features and improve efficiency.

### **B. Isolated Bidirectional DC-DC Converters**

Galvanic isolation between multi-source systems is a requirement mandated by many standards. Personnel safety, noise reduction and correct operation of protection systems are the main reasons behind galvanic isolation. Voltage matching is also needed in many applications as it helps in designing and optimizing the voltage rating of different stages in the system. Both galvanic isolation and voltage matching are usually performed by a magnetic

transformer in power electronic systems, which call for an ac link for proper energy transfer. In the bidirectional dc-dc converters, isolation is normally provided by a transformer (figure 7). The added transformer implies additional cost and losses. However, since transformer can isolate the two voltage sources and provide the impedance matching between them, it is an alternative in those kinds of applications. As a current source, inductance is normally needed in between. For the isolated bidirectional dc-dc converters, sub-topology can be a full-bridge, a half-bridge, a push-pull circuit, or their variations. One kind of isolated bidirectional dc-dc converter is based on the half-bridge in the primary side and on the current fed push-pull in the secondary of a high frequency isolation transformer. The converter operation is described for both modes; in the presence of dc bus the battery is being charged, and in the absence of the dc bus the battery supplies power. This converter is well suited for battery charging and discharging circuits in dc uninterruptible power supply (UPS). Advantages of this proposed converter topology include galvanic isolation between the two dc sources using a single transformer, low parts count with the use of same power components for power flow in either direction. The dual active bridge dc-dc converter with a voltage-fed bridge on each side of the isolation transformer operates utilization of the leakage inductance of the transformer as the main energy storing and transferring element to deliver bidirectional flow power.

An important characteristic of an IBDC is the type of converter at each side. Basically, two types of switching converters can be identified. A current-type (or current-fed) structure has an inductor with stiff current characteristic at its terminals which acts like a current source, like conventional boost converter at its input terminals. A voltage type (or voltage-fed) structure has a capacitor with stiff voltage characteristic at its terminals which acts like a voltage source, like conventional buck converter at its input terminals.

### ➤ **Necessity of Isolations**

Now why we need galvanic isolations in power electronics world? This questions needs to be clarified with the following set of supportive words.

With galvanic isolation, it is possible to eliminate the main forms of interference and the risk of electrical circuit failure when the signal from a sensor is received by the control unit, both in hazardous and non-hazardous areas. Galvanic isolation (named after the Italian physicist Luigi Galvani) is one of the most important techniques of signal conditioning and is both cost effective and easy to implement. It is a technique that aims to resolve issues in implementing a common interface between sensors and control units when the output signals from the sensors differ, whether in their nature (e.g. current, voltage, resistance, etc.), level, or type (e.g. direct, alternating, or impulse current). More specifically, galvanic isolation makes it possible for the signal to flow from the source to the measuring device by way of transformers, opto-isolators, or capacitors.

Galvanic isolation also makes it possible to isolate a low-voltage circuit from the electrical grid (including between two or more circuits in which there is no direct conduction path) and to isolate the power from the control unit, thereby preventing peaks of high voltage and the common-mode high voltage that could destroy the electronic circuits, thereby protecting both users and the measurement and control devices. Isolators make it possible to eliminate the noise induced by the common points of circuits of different potential, while isolating measurement from signal processing.

### ➤ **Types of Isolation**

*Galvanic Isolation* is done by various methods in *power level*. Power level isolations are required to *isolate low power sensitive devices from high power noisy lines* or vice versa. Also, power level isolation provides proper *safety from hazardous line voltages* by isolating the high voltage lines from the operator and other parts of the system. They can be described one-by-one as per following;

#### **1. Transformer**

The popular power level isolator is again a Transformer. There are enormous applications for transformers the most commonly usage is to provide low voltage from a high voltage source.

The transformer does not have connections between primary and secondary but could step down the voltage from high voltage AC to low voltage AC without losing the galvanic isolation.

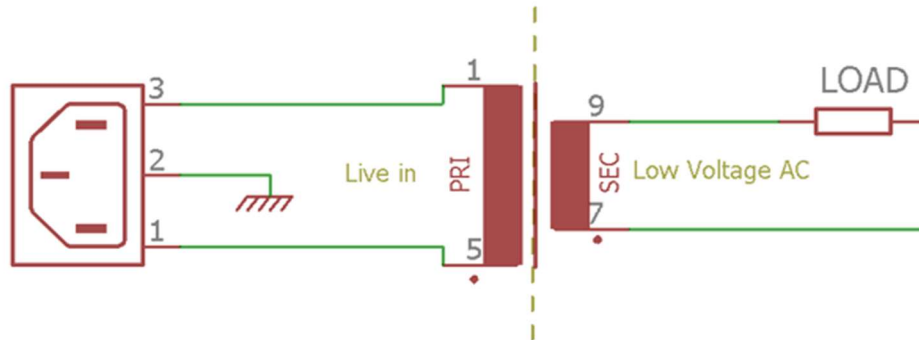


*Fig: - 2 Transformer type galvanic isolation*

The above figure is showing a step-down transformer in action where the primary side input is connected into the wall socket and the secondary is connected across a resistive load. A proper isolation transformer has a 1:1 turns ratio and do not alter the voltage or current level on both sides. The sole purpose of the isolation transformer is to provide isolation.

## **2. Relays**

Relay is a popular isolator with a huge application in the field of electronics and electrical. There are many different types of relays available in the electronics market depending on the application. Popular types are Electromagnetic relays and solid state relays.

An Electromagnetic relay works with Electromagnetic and Mechanically movable parts often designated to as poles. It contains an electromagnet that moves the pole and completes the circuit. Relay creates isolation when high voltage circuits need to be controlled from a low voltage circuit or vice-versa. In such a situation both circuits are isolated but one circuit could energize the relay to control another one.

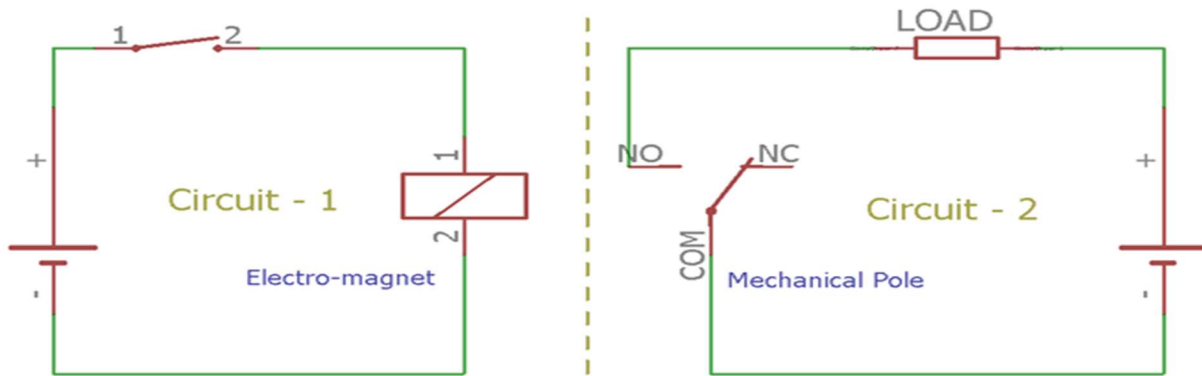
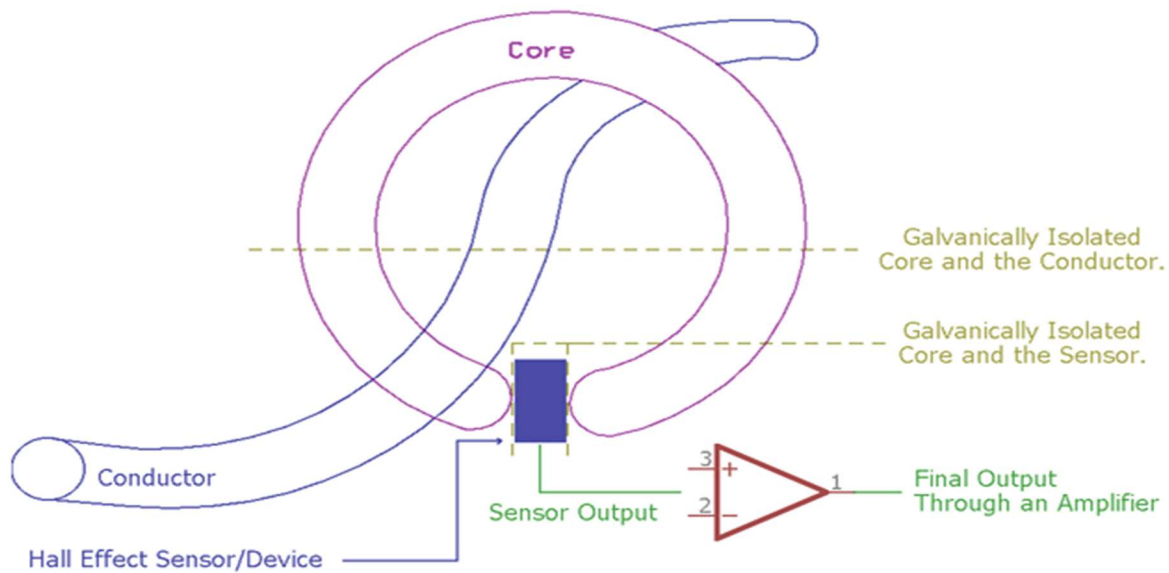


Fig: - 3 Relay type galvanic isolation

In the above figure, two circuits are electrically independent of each other. But by using the switch on Circuit-1, user can control the state of the load on the circuit 2. There are not much *difference between Solid State Relay and electromechanical relay* in terms of working. Solid state relays work exactly the same but the electro-mechanical part is replaced with an optically controlled diode. The galvanic isolation can be build up due to the absence of a direct connection between the input and output of the solid state relays.

### **3. Hall Effect Sensors**

Needless to say that current measurement is a part of Electrical and Electronics engineering. There are different types of current sensing methods available. Often the measurements are required for High voltage and High current paths and the value read has to send to a low voltage circuitry which is a part of the measurement circuit. Also from the user perspective, invasive measurement is dangerous and impossible to implement. Hall Effect sensors provide *contactless current measurement* accurately and help to measure the current flowing through a conductor in a non-invasive way. It provides proper isolation and ensures safety from hazardous electricity. Hall Effect sensor uses electromagnetic field generated across the conductor to estimate the current flowing through it.



*Fig: - 4 Hall effect Sensor*

The core ring is hooked over a conductor in a non-invasive way and it is electrically isolated as shown in the figure above.

### **Applications**

The applications of galvanic isolation include the following.

- Galvanic isolation is an extremely important parameter and the application of this is enormous. It is used in industrial, consumer goods, medical, and in the communication sector.
- In electronic industries, this kind of isolation is used for power generators, measurement systems, distribution systems, I/O logic devices & Motor controllers.
- In the medical field, this is one of the main priorities used in the medical equipment which can be connected directly through the bodies of patients like Defibrillators, Endoscopes, ECG & different types of imaging devices.
- These are used in communication systems at the consumer level. The examples are routers, Ethernet, switches, and many more. Standard consumer goods such as SMPS,



chargers, logic boards of computer are the most frequently used devices which employ galvanic isolation.

### ➤ **Types of DC-DC Converter**

Different types of DC–DC converters for renewable energy and other innovative applications and storage to enhance efficiency simultaneously overcoming the drawbacks of converters. DC–DC converters are classified into three major technologies based on their operation modes- 1) linear mode, 2) hard switching mode, and 3) soft switching mode.

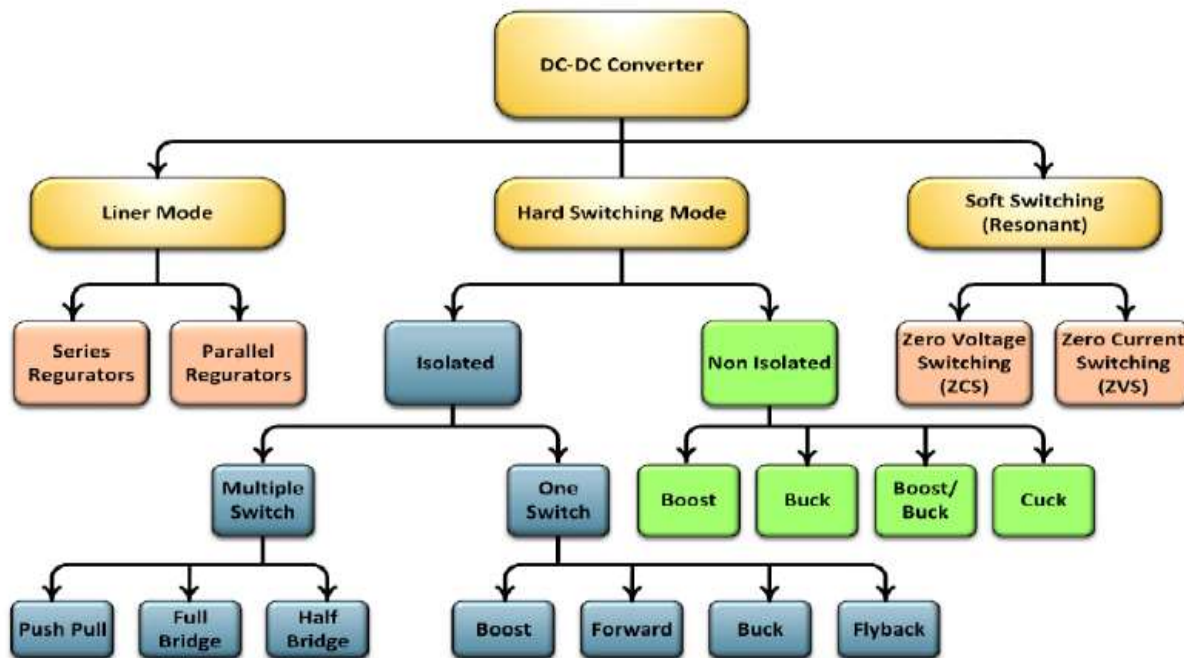


Fig 5: - Classification tree of DC-DC Converter

- ❖ **Linear mode:** It has features such as simple structure, low noise generation with good regulation, and faster response. On the other hand, its drawback is low efficiency due to power losses in various operating conditions.
- ❖ **Hard switching mode:** It converters are sub-divided into non-isolated and isolated converters based on galvanic isolation. The buck, boost, buck–boost, and Cuk converters are

examples of the hard switching mode topologies and these are without isolation (non-isolated) and identified as **chopper** circuits. However, isolation (transformer) is necessary for safety causes when the converters are supplied by the utility grid. Power converters along with their control techniques, help regulating voltages of nodes under micro grids with different types of loads such as resistive, linear, non-linear, inductive, constant power loads etc.. The drawbacks of hard switching mode converters include high electromagnetic interference (*EMI*), high switching losses, and bulky size and weight, which affects the switching frequency in addition.

❖ **Soft Switching Converter:** In the field of Power Electronics Technology, another technology has been arrived that is *Soft Switching Converter*, in various topology, which has obtained a milestone success through its implementation as well as application by means of multiple factors like switching loss reduction, power density improvement, minimization of EMI i.e. Electromagnetic Interference, reducing the overall size of converter w.r.t to its hardware structure and space-taking tendency. In the past few decades, quite a number of topology related to this soft-switching converter, either *in ZVS (Zero Voltage Switching)* or *ZCS (Zero Current Switching) mode*, had been reported towards many authorized organizations. This documentation will review effectively on various soft-switching techniques based on *resonant network location* (arrangement of Inductor and Capacitor in different style), *performance characteristics, dynamic analysis and the working principle with the functioning of different components*. Also besides it, some innovating and world-wide accepted applications, its limitations and drawbacks are also depicted. this converter utilizes more than one switching method converter, including half-bridge, full-bridge, dual half-bridge, fly back, and push–pull converters

➤ **Merits and demerits of DC-DC Converter:**

➤ **Merits:**

- It simplifies the power supply systems in the circuit.
- It provides isolation in the primary and secondary circuits from each other.
- It provides a technique to extend potential (voltage) as required.

- It is available as a hybrid circuit with all elements in a single chip.
- It is also used in the regulation and control of DC voltage.
- The output is well organized as positive or negative.
- Battery space can be reduced by using a converter.

➤ **Demerits:**

- Switching converters lead to more noise.
- They are expensive as an external circuit is required.
- Choppers are inadequate due to unsteady voltage and current supply.
- More ripple current, More input and output capacitance, higher losses, etc.

➤ **Necessity of Soft Switching**

UPS (Uninterrupted Power Supply) used Computers, renewable energy sources, and auxiliary power supplies used in all types of vehicles need a DC-DC Boost Converter having a high gain, but due to narrow duty cycle feature, such requirements can't be met easily. Achieving a high gain using a PWM (Pulse Width Modulation technique) technique is also not a proper solution because of the *fast transition of voltage ( $\delta v/\delta t$ ) and current ( $\delta i/\delta t$ )* that occurs across the power switches (*MOSFET, IGBT, THYRISTOR, etc.*) and this may lead to generation of Electromagnetic Interference noise, which may be exceeded its boundary limits in the power lines.

On the other hand, power dissipation will occur in the switches due to that transition in operational states, during turning ON and OFF actions, from the existing voltage and current values. Due to the demand of low sized converter and high power density within it, a serious effect can be noticed with these converters on the electrical power system as they generally operate at high switching frequency (nearly within 50 kHz – 200 kHz), and moreover if we go to decrease the power dissipation at switches (which is treated as loss) then automatically power density will be improved.

That's why, *soft switching techniques with high-frequency* are very much useful in case of avoiding the negative impact of EMI problems, switching loss and low efficiency; and also useful

for obtaining the converter low size, high power density, high reliability and components with lower ratings. As a result, any topology would be very much cost-efficient.

Soft Switching techniques contains high frequency resonant network (generally a power oscillating component comprising with Inductor and Capacitor i.e. LC Circuit) are added with hard-switching circuit in order to make the switching waveform worth of minimizing switching losses, EMI problems and switching stress.

- **Resonant Converter**

Now let us talk about a brief theory of Resonant Switch Converter (*as per our project, because also there exists Resonant Load Converter which is scope beyond this paper*). These converters are of three types- **1) Series**, **2) Parallel** and **3) hybrid** (Combination of series and parallel), where a series capacitor is connected across the power switches (eventually with its internal snubber resistances) and resonant inductor in series with power switches. These switches are in the form of non-isolated series resonant network, or isolated series resonant converter (Isolation is carried out by means of either proper isolation transformer or using a tap-changing transformer with 1:1 tap setting). *Parallel isolated Converter* consists of a parallel capacitor across the switch and transformer to provide ZVS type of operating mode and in case of series isolated converter, more than one elements are needed at that parallel location.

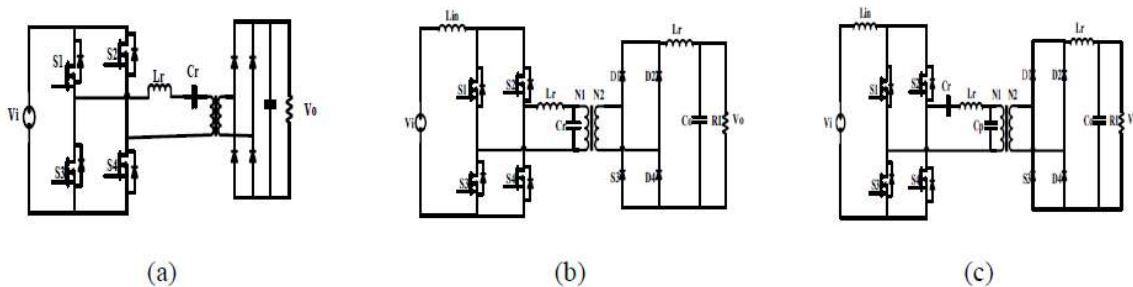


Fig 6: - (a) Series Resonant Converter, (b) Parallel Resonant Converter, (c) Hybrid Resonant Converter

Due to the fact that, in series resonant converters, resonant elements are connected in the primary power path, subjecting the resonant inductor to bidirectional voltage. As a result in generating additional voltage impact on the power switches. In addition, conduction losses are

substantially increased due to significant amount of circulating energy as a result of all power flowing through the resonant inductor. However, in parallel resonant converter, the shunt resonant circuit is activated for partial resonance to execute ZVS or ZCS during ON and OFF transition. Consequently, the circuit regressed back towards PWM operating mode after switching transition. Below, a general block diagram of resonant converter is given at *figure 3* and isolation scheme with the help of a **1: N** transformer (generally  $N=1$  i.e. isolation transformer) is shown in *figure 7*.

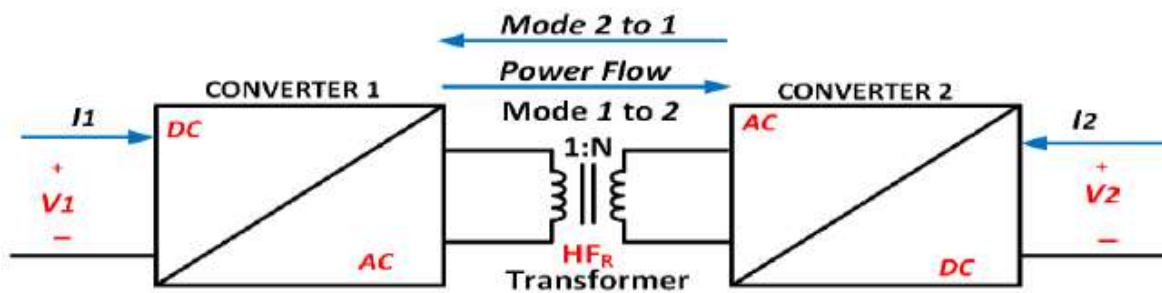


Fig 7: - Structure of an isolated bidirectional converter with a transformer

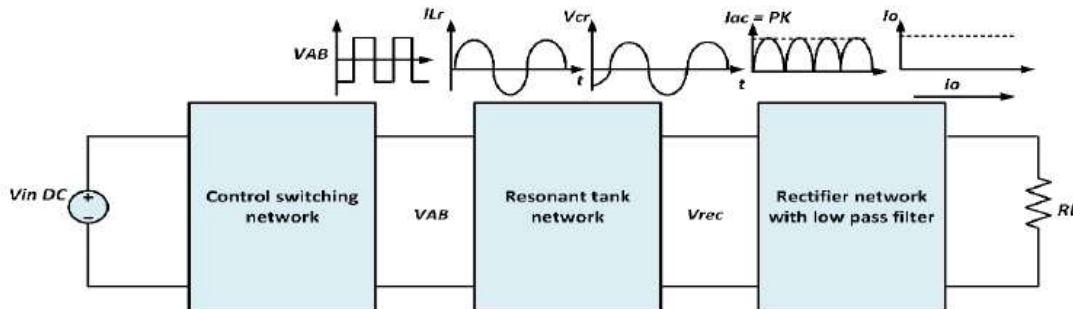


Fig 8: - General Schematic block diagram of a resonant converter

Now let us discuss about its two types of switching methods as per following;

- **Zero Voltage Switching (ZVS):** Basically, in ZVS, switching occurs at the initial no-voltage condition of the turn-on device, by making the switch voltage zero and retarding the voltage rise by creating a time delay for the current so that current transition occurs at the

zero-voltage state. ZVS banishes capacitive turn-on loss, and reduced switching losses at overall. The topologies of which can be either isolated type to achieve electrical isolation and voltage scaling or non-isolated type. A ZVS for a bridgeless power factor correction (PFC) boost converter operating in CCM i.e. continuous conduction mode, this provides ZVS for the switches and reduces switching losses. Similarly, the heat controlling problem, which is associated with conventional diode rectifier has been turned around due to the controlled transition in the output diode current at turn-off. These converters depend on soft switching for high-efficiency operation.

- **Zero Current Switching (ZCS):** ZCS reduce switching losses at turn-off by bringing the switch current to zero forcefully, before the voltage between drain and source side increases from zero to turn-off static value. ZCS at turn-off makes the convenience for removing the stored charges which might cause a long current Rump. This feature makes ZCS highly preferable. However, the majority of the ZCS topology usually involved in reducing switching losses against the increase conduction losses. This is due to high circulating energy caused by the inductor in series with the power switch. This action leads to exposure of the power switch to a high current stress and a diode to high voltage stress. Besides that, another limitation of ZCS is the harmful parasitic nature of the power switch in terms of unnecessary electrical energy taking tendency. As a results of non-utilization of the output capacitance of the power switch, the capacitance attains oscillation with the resonant inductor when the switch turn-off. The low frequency parasitic ringing causes significant switching loss, noise and increment in voltage stress of the power switch. In addition, ZCS operates with constant on-time control.

ZCS are more effective in IGBT switching losses reduction than ZVS specifically at low frequency ranges and high power application.

In addition to *DC–DC* conversion, *DC–AC conversion* (Inverter operation) is also required to supply AC loads as well as grid integration *multilevel inverters* are one of the most crucial power converter topologies in industrial and residential applications. In recent years, multilevel inverters have achieved a lot of contemplation in the applications of medium voltage and high-

power ranges due to their multi-angled advantages, and some of the advantages of multilevel inverters over the conventional two-level inverters include lower *EMI*, lesser harmonic distortion, and lower voltage stress on semiconductor elements. They require a greater number of semiconductor elements (mainly switches) and for this drawback the system becomes unnecessarily bulky and budget overloaded. When compared to two-level inverter topologies with the same power ratings, multilevel inverters are more effective in eliminating the harmonic ripple component of voltage and current waveforms. Multilevel topologies are classified into different types, such as cascaded h-bridge ('h' stands for hybrid), diode clamped, and capacitor-clamped inverters. In the applications requiring high-power converters, multilevel inverters are essential. They are also widely used in energy sources which are substantially environment friendly, where they serve as an interfacing link between renewable energy sources, such as *PV* modules, and high-power loads. Among the common application areas, these inverters are *Flexible Alternative Current Transmission System (FACTS)* devices, power converters, and reactive power compensation systems for high-power *AC* motors. Apart from these, recently the hybridization of topologies is becoming famous in various industries. For an example, resonant converters are enabled to operate in *bidirectional mode* for power transfer through both ways (from Low Voltage to High Voltage and vice-versa). Bidirectional resonant converters are relatively easy to integrate amongst other components. Thus, they are widely used in *battery chargers, electric vehicles, high-voltage power supply applications, and renewable energy systems.*

# **Chapter 2**

## **(Literature Review)**



## ▪ **Literature Review:**

A soft-switching bidirectional DC/DC converter with a LCLC resonant circuit is proposed that has the dual advantages of isolated converter and non-isolated converter. In boost mode, high efficiency can be achieved at high boost ratios. In buck mode, the circuit can also achieve automatic voltage equalization of full-bridge capacitors. In this study, a detailed theoretical analysis of the LCLC structure is performed, and the specific operating modes of the circuit in buck and boost mode are given. The circuit modes of the soft-switching resonant process are quantitatively analysed. The GSSA (generalized state space averaging) method was used to model and control the system. According to the obtained transfer function, the PID control circuit of the system is designed by using the zero-pole cancellation method, which enabled the system to obtain superior control performance. A prototype of 1000W was made, and the experimental results are in good agreement with the theoretical results.

In recent years, there are mainly two aspects in the research of bidirectional converters. One is the improvement of the topological structure. Through the analysis of the topological structure of the bidirectional converter, some applicable topological structures for special conditions are proposed. The second is the study of control strategies. Since bidirectional converters need to operate in different modes and the corresponding models of different modes are not the same, it is necessary to propose corresponding control strategies for different operating modes of bidirectional converters.

### **1. Converter with HVDC & LVDC implementation**

Converters with bidirectional capability for *MEA (More Electric Aircraft)* and *AEA (Antenna Electronics Assembly)* applications is a current research topic. Bidirectional power converters are linked to power management in aircraft applications as part and parcel manner, with *Electrical Storage Systems (ESS)*. Such ESS can be present in buses with regenerative loads, or in micro grid electrical distribution architectures, in which *generators operate in parallel* and *sources and loads are balanced by means of ESS*. Micro grid architectures are considered a promising alternative to one-generator for a single-bus conventional electrical architectures, as

it is expected to lead to generators size reduction. As for example, a bidirectional power converter for  $270 V_{DC}/28 V_{DC}$  is investigated, with a focus on control capability of different energy storage sources (multiport converter). In this context, high-voltage DC (HVDC) to low-voltage DC (LVDC) bidirectional converters have been proposed *as inter-connecting component between HVDC and LVDC buses* in pure HVDC architectures. Bidirectional capability might also be used to increase system redundancy. For example, in aircraft emergency operation in which HVDC source is not available, they may operate in boost mode to feed critical loads from LVDC bus.

In the above context, the key aspects of the design of power converters are under prime observation which are enabling bidirectional power transfer between a HVDC network and  $28 V_{DC}$  buses used in power electronics related to aircraft application. As per the fact that power converter should be able to generate either LVDC or HVDC voltages (operation in buck or boost modes respectively), and to transfer power under the presence of an externally generated HVDC or LVDC bus; the multi-angled features of converters are under crucial target. Internal current control capability is expected to facilitate control with this type of arrangement. In particular, we will focus on suitable topologies for near about 3 kW bidirectional isolated power transfer between  $270 V_{DC}/28 V_{DC}$ . This comparative study is the first design step of a modular converter design, in which power capability can be extended to up to 20 kW by means of parallelization, and compatibility with  $\pm 270 V_{DC}$  voltages by means of series/parallel modules connection. It is interesting to note that in such modular solution, the performance of the modular connection is very close to the performance of the single modules that we have considered in this study, at least in terms of efficiency and power density. Although modules nominal rating in the HVDC side is  $270 V_{DC}$ , results of achievable performances in a  $\pm 270 V_{DC}$  distribution network can also be extrapolated from the results of this study, which make this comparative study valid for any voltage level of the HVDC distribution network. As a final remark, an optimized design of a  $270 V_{DC}$  module will outperform a wide range module in the complete range of  $270 V_{DC}$  to  $540 V_{DC}$  HVDC voltage range, since wider operation ranges always involve degraded performances. Since aeronautic stringent requirements requires a high

degree of optimization, it have been decided to limit voltage range as much as possible, respecting voltage ranges defined in MIL-STD-704 standards.

## **2. Converter in DAB & MEA topology**

Several topologies have been proposed as suitable solutions for the literature review purpose. Typically, one of the widely implementable and preferable topologies for isolated bidirectional power transfer is *Dual Active Bridge (DAB)* [2]. For this topology, the simplest modulation scheme is the so called phase shift modulation [3], in which the phase shift between the two full bridges (operating at maximum duty cycle) is controlled. There are many alternative modulation schemes have been proposed for DAB to improve its performance. In [4, 5], the so called dual-phase-shift is presented as an alternative to phase shift modulation. In [2, 6], a general study of all modulation possibilities of DAB is presented, and their capability in terms of efficiency and power density is experimented in a 2 kW isolated automotive application, under a wide operation range. The design, which implements the so called Extended Triangular Trapezoidal (TT) modulation, is stated as a guaranteed solution, in terms of efficiency, power density and modulator simplicity. In [2], DAB optimized converter is compared with other suitable topologies such as the *bidirectional current doubler (CD)* topology [7], three phase dual active bridge [8] and bidirectional LLC (operating at fixed switching frequency, as in [9]). All the topologies Energies 2020, 13, 4883; 3 of 27 are optimized for wide range operation as well, and they are included in the topology comparison in terms of *efficiency and power density*. However, the comparison in [2] does not consider the impact of including recent WBG (Wide Band Gap) semiconductors in the design improvement.

As an alternative to voltage sourced DAB based topologies, current sourced topologies also bring to us a set of apt solutions for isolated bidirectional applications. An extensive review of the state of the art of isolated bidirectional current fed topologies and modulation schemes is executed in [2], for renewable energy applications ( $20 V_{DC}$ – $40 V_{DC}$  to  $400 V_{DC}$ , 2 kW). A topology comparison based on optimized modelled designs performance is carried out. As in [10], a large set of topologies are compared under the similar operating conditions, and a weight

comparison is also executed. Still, efficiency performance is only reported for boost operating mode, and no information is provided about efficiency variation with load or voltage.

No extensive topology and modulation comparison have been carried out for HVDC/LVDC bidirectional MEA applications. However, several topologies have been proposed for this particular application, and non-exhaustive topologies comparisons have been carried out in the literature. As an example of MEA application, in [11], several topologies for bidirectional  $270 V_{DC}/28 V_{DC}$  power conversion have been investigated. DAB (with phase shift modulation) shows the most promising results based in the simulations. A 1.2 kW DAB SiC (HV)/Si(LV) demonstrator based on this topology is developed, with a maximum measured efficiency of  $\sim 93\%$  at half load, and efficiency  $\sim 90\%$  at full load. Switching frequency is 100 kHz.

Several bidirectional HVDC/ $28 V_{DC}$  converter prototypes for MEA application are presented in [12]. A 1 kW DAB prototype, switching at 24 kHz was built, with achieved efficiencies of 95.8% at half load, and 94.4% at full load. Also, a 10 kW Series Resonant converter was built, with high efficiencies of 98% at nominal load. However, these high efficiencies come at the expense of a low switching frequency (20 kHz), which might lead to low power densities (not available data regarding weight). Finally a 20 kW Quadruple Active Bridge (as in [13]) prototype is also presented in [12], with nominal efficiencies of 98%, although no information is provided about switching frequency or power density.

Finally, a novel topology for the particular application studied here is presented in [17]. This topology, referred to as Active Bridge Active Clamp (ABAC), is an alternative to DAB phase shift topology. ABAC is a DAB variant with floating DC links on the LV side, and interleaved LV DC inductors. The ABAC architecture features inherent current control capability, very low LV output ripple, and short circuit current control capability. Although DAB and DAB-3p inherently lack these desirable capabilities, a filter and control structure such as the proposed in [2] would enable them. The comparison in [17] neglects the consideration of a more favourable filter structure for DAB.

### ***3. DC-DC Converter Current Doubler Topology***

In [15], they optimize a bidirectional 10 kW 540 V<sub>DC</sub>/28 V<sub>DC</sub> bidirectional multi-cell converter, which can be seen as an extension to 'n' phases of bidirectional current doubler topology [2]. They successfully implement GaN MOSFETs in LV switches, taking advantage of low currents per phase due to the large number of phases. In [16], two possible solutions are proposed for the same application as [15]. First, a parallelization of interleaved 3 kW modules (phase shift full bridge, with push pull in LV side) is developed. Then, a multi-cell architecture is proposed to achieve better performance than in the modular solution. Summing up, although the achieved performance in [15, 16] prove suitability of multi-cell topologies for a MEA application, their scope differs from the targeted modular approach of this study, in which lower power and voltage rated converters can be configured in series/parallel configurations.

### ***4. Super-lift LVO converters for EV applications***

As there is a huge growth in industry of Electric Vehicles (EVs) in recent years and also due to higher penetration of renewable energy resources like Photovoltaics (PV) incorporated with DC-DC multi-port converters (MPCs) with wide-voltage range that has come as a burning topic. A totally new generation of MPCs is applied in technology such as EVs and RESs (Renewable Energy Sources) The main advantage of these MPCs is, there is no need of electro-magnetic devices. The study related to this topic has brought a new approach to construct a MPC by integrating two separate SIMO (Serial Input Multi Output) Converters resulting in a reduction of the number of elements, thus making it less bulky and cost-efficient.

DC-DC resonant converters with two isolated outputs to be used in EV's application. In this suggested structure, a half-bridge DC-DC Converter with split capacitor, was used to reduce the size of converter.

Now by observing the gaps in the previous works, a new structure is introduced for the MPCs, which has some features such as generating two different step-up and step-down outputs within a considerable range, low ripples in the output voltage and not dependent on any electromagnetic components. So, a DC-DC multi-port converter is introduced by integrating or

combining a Super-lift LUO and a Buck converter. In this proposed topology, the Single Input Dual Output (SIDO) converter has the advantages of positive super-lifted while simultaneously generating step-up voltage by LUO converter and step-down voltage by the Buck converter.

Meanwhile, the introduced SLBC (Super-lift and Buck Converter) has a simple structure and an appropriate control method providing a wide range of output voltages. Also the simulation and experimental results indicate a considerable and significant reduction in conduction losses compared to other SIDO converters in the same specifications and constraints. The operational accuracy is validated by performing several simulations in software like PSCAD, EMTDC etc. and testing a 150 W prototype in the laboratory. Accordingly, simultaneous step-up and step-down outputs can be varied from about 98% to 93% by increasing the output power. The proposed structure is applicable to a SIMO converter with different output.

### ***5. SPWM inverter for Digitized Signal Generation***

Relevant studies in the field of Photovoltaic Power generation systems, three level inverters are widely used. In the present time, control technology of three-level inverters mainly focuses on Pulse Width Modularised control strategy, Harmonic suppression and DC Bus voltage balance control. Utilization ratio of the DC bus voltage is the key point in optimizing the pulse width modulation algorithm. In such cases, three level inverter's pulse width modulation algorithm is basically relies upon SPWM i.e. *Sinusoidal Pulse Width Modulation* technology. IN SPWM method, the harmonic content present in power signal waveform is reduced by using natural sampling method.

By realizing super modulation function, it can also make up for the deficiency low utilization ratio of DC bus voltage in SPWM. Therefore, it is reasonable and feasible to choose SPWM as PWM algorithm of three-phase inverters in high voltage high-power situations.

Digital Signal Processor equipment and a polynomial expression determining method has been used to realize to the digitisation of natural sampling method in SPWM. But the DSP chip faces the problem of insufficient ports which limits the size of the expression that means higher order expressions can't be handled with this traditional method. To mitigate this problem of port

insufficiency, large scale logic equipment consisting of improved security and stability, are used to realize the desired pattern of digitization in natural sampling process. Its sinusoidal signal is generated by Analog circuit, sampled by microprocessor and then transmitted towards Field Programmable Logic Device (FPLD chip) which completes the digitization of triangular carrier wave.

In high power applications, the switching frequency is low in general and the natural sampling SPWM will further improve the output waveform quality. Also besides this, the DC Bus voltage balancing will also be improved in very efficient manner. But still the concerned technology related with this needs to be modified for the sake of today's modern industrial strategy.

For some crucial drawback mentioned above, the theory of three-level natural sampling method in SPWM and all attached digital technologies are needed to be re-studied for implement on FPGA based chip to realize it. Here in this literature section, a complete digital framework of SPWM with natural sampling are completely reviewed. Here, an ultra-relational and comparative calculation method is proposed to realize the advanced calculation of sampling points. Digital natural sampling method always avoids the cases like Taylor Series expansion or convergence judgement in traditional calculative strategies.

In FPGA, since Sine wave, Triangular Wave and any synchronized signal are automatically generated, which helps further improvement of the digitization degree, pulse width control accuracy and system response speed. The experimental results show that harmonic content of the SPWM output waveform using digital natural sampling method is lesser than 5-15% than that of the symmetrical regular sampling method. That's why the concerned sampling method is superior to the conventional symmetrical one with respect to harmonic content. And this digital sampling process can further improve the shape, quality and stability of DC Bus voltage balancing scheme.

## ***6. SPWM with Carrier frequency Modulation***

Relevant studies in SPWM Single-phase Inverter are also there in which the carrier frequency is modulated twice. In such inverters whose switching devices are working on Sinusoidal Pulse

Width Modulation (SPWM) mode, the frequent ON-OFF procedure of the switches is the primary sources of Electromagnetic Interference (EMI). The EMI level can especially arise up to the peak magnitude at switching frequencies as well as its harmonic frequencies. Sinusoidal Pulse Width Modulation method is used to control the EMI in the inverter output *and Carrier Frequency Modulation (CFM)* is the best scheme to suppress the EMI effect. Here, the peaks of interference can be effectively reduced by using CFM method.

The above scheme is generally performed in order to analyse the spectrum of the output voltage of differential mode in a SPWM inverter with periodic CFM technique. Using periodic CFM, it can reach peak suppression with smaller frequency distortion. This kind of CFM scheme makes the frequency of PWM triangular carrier frequency vary with the fluctuation of a periodic signal but its disadvantage of periodic modulation lies in its discrete spectrum where the frequency of periodic signal is higher, energy of the spectrum would be focused too on discrete spectral lines for handling the interference peaks. Moreover, using differential periodic signals will obtain different effects of interference peak suppression.

To solve these problems, the scheme of *Modulating Carrier Frequency Twice (MCFT)* is proposed. In this scheme, the frequencies and waveforms of the *first and second modulated signals can be optimized to form a new synthetic modulation signal*. The simulations performed on it prove that using the synthetic signals brings the best effect of the interference peak suppression while *the maximum frequency deviation of CFM is fixed*. Also the feasibility and validity of the scheme has been proved by simulation and experimental results in a single phase inverter.

Although the scheme of MCFT is verified only in the single phase inverter but it is a suitable process for suppressing interference peaks generated at carrier frequency signals in other converters which are triggered and controlled by PWM or SPWM and it can further also be useful in other methods like *multiple CFM*.



## **7. Multi-level inverter with SPWM Control**

Relevant studies in the field of existing multi-level inverter circuit is being done and coming up with a modified multi-level inverter with step-up operation using fewer components is proposed here. The proposed circuit, under concern, consists of three capacitors and eight switches, which can able to produce seven-level output, but one thing is noticeable here that, more no. of switches decreases the converter efficiency. *Charge Pump* principle is based on for boosting operation *about 1.5 times* of the input voltage as output. In 5 level inverter, capacitor-based charge pump strategy is employed where charging of capacitor is possible in parallel connection, but discharging of it occurs at series connection. Some seven-level inverters are using diodes multi-level inverters which affects the efficiency of converter and voltage boosting performance is not in desired and required level.

An SPWM is employed is employed to trigger the switches, and the switching pattern is mainly focused to balance the capacitors and their charging and discharging rate also. Using some mathematical in some Engineering based Simulation software like SIMULINK (under MATLAB), the seven level software is validated in the real time model. The main purpose of such multi-level circuitry is to reduce the total harmonic distortion.

## **8. DC-DC Converter with several application based topologies**

**Hua Bai et al.**, conducted a study on bi-directional DC-DC converter in a HEV. This DC-DC converter is a high-power converter that links the high voltage battery (HV) at a lower voltage with the high voltage DC bus. The typical voltage of a battery pack is designed at 300 to 400V. The best operating voltage for a motor and inverter is around 600V. Therefore, this converter can be used to match the voltages of the battery system and the motor system. Other functions of this DC-DC converter include optimizing the operation of the power train system, reducing ripple current in the battery, and maintaining DC link voltage, hence, high power operation of the powertrain.

In [18], a *zero voltage switching (ZVS) bidirectional isolated DC-DC converter* was formulated. This is used in high power application especially for power supply in fuel cell vehicles electric

vehicle driving system and power generation where a high power density is required. This technique has the advantages of low cost, light weight and high reliability power converter where the power semiconductor devices (MOSFET, IGBT, etc.) and packaging of the individual units and the system integration play a major role in isolated DC-DC converter hybrid/fuel cell vehicles.

In [18], a novel integrated bidirectional ac-dc charger and dc-dc converter (henceforth, the integrated converter) invented for PHEVs and hybrid-plug-in-hybrid conversions is proposed. The integrated converter is able to function as an ac-dc battery charger and to transfer electrical energy between the battery pack and the high-voltage bus of the electric traction system.

In [18], the basic requirements and specifications for PHEV bidirectional ac-dc converter designs were presented. Generally, there are two types of topologies used for PHEVs: an independent topology and a combination topology that utilizes the drive motor's inverter. Evaluations of the two converter topologies are analysed in detail. The combination topology analysis is emphasized because it has more advantages in PHEVs, in respect to savings in cost, volume and weight.

It was proposed in [18] about multi-power-port topology which is capable of handling multiple power sources and still maintains simplicity and features like obtaining high gain, wide load variations, lower output-current ripple, and capability of parallel-battery energy due to the modular structure. The scheme incorporates a transformer winding technique which drastically reduces the leakage inductance of the coupled inductor.

In [18], a bidirectional DC-DC converter is designed for a small electric vehicle. The DC-DC converter designed and tested is capable of raising the voltage from the battery pack (96 V nominal) to 600 V necessary to feed the Variable Frequency Drive that controls the induction motor. This converter is also capable of working in the opposite direction (600 V to 96 V)

# Chapter 3

## (Working Principle)

- *Working Principle*

Now the working strategy of the whole system can be highlighted in two subcategory. Firstly, it can be depict the working principle of Low-Voltage to High-Voltage Conversion and vice-versa

through the *DC-DC Soft-switching converter* and secondly, the working procedure of a *SPWM (Sinusoidal Pulse Width Modulation) Inverter* to get AC Power output for the Asynchronous Induction Machine load.

### **(i) DC-DC Soft Switching Converter: -**

In this concerned bi-directional (with galvanic isolation) resonant DC-DC converter,  $V_L$  indicates the low-side voltage of the converter, whereas  $V_H$  indicates high-side voltage of the circuit. The soft-switching cell consists of two resonant inductors  $L_{r1}$  &  $L_{r2}$  and a resonant capacitor  $C_p$ . This three components together form a resonant impedance gain link. The capacitor  $C_d$  is an auxiliary capacitor of the circuit, which is connected to the parallel of MOSFET switch-arrangement at the low-voltage side, as well as parallel with transformer. That  $C_d$  and the half-bridge capacitors  $C_1$  &  $C_2$  maintain the equalized partial voltage of the half-bridge circuit, to mitigate the problem that half-bridge voltage division is not equal, caused by half-bridge capacitors that are participating in resonance.  $C_d$  provides a stable half-bridge voltage output and maintains the continuous operation of the converter by maintaining the  $dv/dt$  at a certain specific boundary. Now we can shortly describe the two modes of power conversion; boost mode and buck mode.

**(a) Boost Mode:** Before diving into the boost mode operation, the working principle of a simple boost converter have to be depicted in the following manner.

**Definition:** A boost converter or a DC boost chopper is another name for a DC boost converter. It's a DC-DC converter that can boost voltage and has a greater output (load) voltage than the input (power) voltage. A switching power supply containing at least two semiconductor elements (a diode and a transistor) and at least one energy storage element is known as a boost converter (inductor). Filters built of capacitors (and occasionally inductors) are positioned at the input and output ends to reduce voltage ripple. It's used in a variety of applications, including automotive applications, power amplifier applications, adaptive control applications, battery power systems, consumer electronics, communication applications, battery charging circuits,

heaters and welders, DC motor drives, power factor correction circuits, and distributed Power architecture systems.

**Operation Principle:** The tube that controls the power switch. The pulse width modulation (PWM) signal controls the  $V_T$  of the boost DC-DC converter, which is analogous to a mechanical switch that closes and opens at a high speed. Figure 9 depicts its functioning principle. Figures 9(a) and 9(b) depict the present routes when  $V_T$  is turned on and off, respectively. The figure depicts the closure and opening of switch  $S$  to aid circuit analysis. It takes the place of  $V_T$ 's on/off switches.

When  $V_T$  is switched on (i.e.,  $S$  is closed), the input voltage  $U_i$  is applied straight to both ends of the energy storage inductor  $L$ , and the freewheeling diode  $V_D$  is turned off, as illustrated in Figure 9(a). Because the voltage of  $U_i$  is applied to  $L$ , the current  $I_L$  of the inductor increases linearly, as does the energy stored in the inductor. The inductor's induced electromotive force is left "+" and right "-." During this time, the energy provided by the input current (i.e., the inductor current  $I_L$ ) is stored as magnetic field energy in the energy storage inductor  $L$ .

The filter capacitor  $C$  is discharged at the same time to give a current  $I_o$  for the load  $R_L$ , and the capacitor  $C$ 's discharge current  $I_1$  is equal to the load current  $I_o$ .

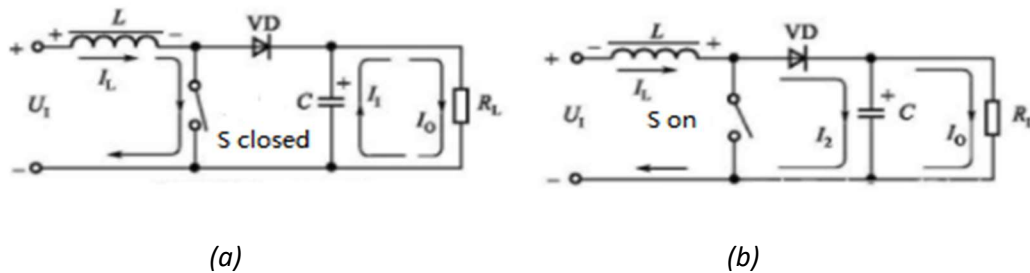


Fig: - 9 (a) Current path when  $V_T$  is on, (b) Current path when  $V_T$  is off

Because the inductor current cannot vary abruptly when  $V_T$  is switched off (i.e.  $S$  is disconnected), an induced voltage of left "-" and right "+" is generated on  $L$  to preserve the inductance, as shown in Figure 9(b). The present  $I_L$  remains unchanged. The freewheeling diode  $V_D$  is turned on at this point, and the induced electromotive force on  $L$  is connected in series

with  $U_1$ , converting the magnetic field energy stored in  $L$  into electric energy, which provides current to the load at a voltage greater than  $U_1$  and charges the output filter capacitor  $C$ . The total of the capacitor charging current  $I_2$  and the load current  $I_0$  is the inductor current  $I_L$ .

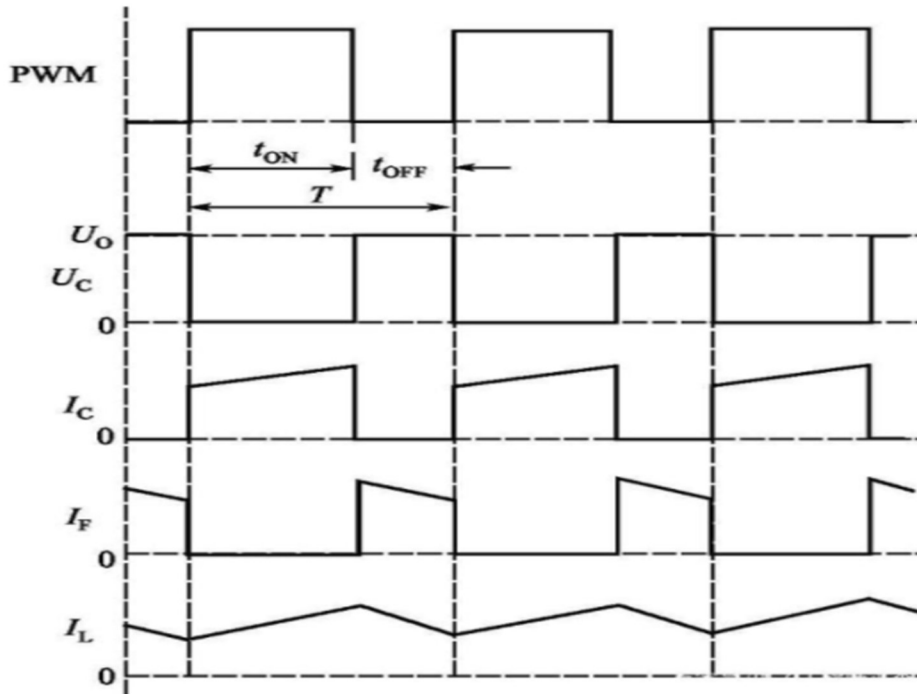


Fig 10: - Voltage and current waveforms of a DC/DC Boost converter

Figure 10 depicts the boost DC-DC converter's voltage and current waveforms. PWM is the pulse width modulation waveform,  $t_{ON}$  is the power switch  $V_T$ 's on time, and  $t_{OFF}$  is the power switch  $V_T$ 's off time. The switching phase is denoted by the letter  $T$ . The power switch tube  $V_T$ 's collector voltage waveform is denoted by  $U_C$ . The collector current waveform of  $V_T$  is  $I_C$ . The current waveform of the boost diode  $V_D$  is  $I_F$ , and the current waveform of the inductor is  $I_L$ . When the power switch tube  $V_T$  is turned on, the collector voltage  $U_C$  is zero; when the power switch tube  $V_T$  is turned off, the collector voltage  $U_C$  is equal to the output voltage  $U_O$ . The inductor current increases linearly during the  $V_T$  on-time of the power switch and falls linearly during the  $V_T$  off-time. The collector current  $I_C$  of  $V_T$  and the current  $I_F$  of the boost diode  $V_D$  combine to create the inductor current  $I_L$ .

Here in this topology of project (figure 15), electrical energy flows from the lower energy storage terminal  $V_L$  to the high-voltage side DC bus,  $V_H$ . When the electrical energy flows into the converter, the inverter circuit (which is the intermediate functional division of this topology) composed of the switching transistors  $S_1$  and  $S_2$  is inverted into an AC square wave with amplitude  $V_L / (1-D)$  [ $D = \text{duty cycle} = T_{\text{on}} / T_{\text{off}}$ ], and the AC pulsating wave flows into the LC-LC resonant circuit, and then flows into a voltage raising rectifier circuit, composed of switching transistors  $S_3$  and  $S_4$ , and finally reaches the voltage  $V_H$  on the high voltage side. During the boost mode, the main inductor  $L$  maintains the circuit in a continuous current state, through controlling  $di/dt$ , means current changing rate.

**(b) Buck mode:** As similar to the boost mode, before diving into the buck mode operation, the working principle of a simple converter have to be depicted in the following manner.

**Definition:** A buck converter (buck converter) is a DC-to-DC power converter that lowers the voltage from the source to the load (in drawing a smaller average current). It's a type of switching power supply (SMPS) with at least two semiconductors (a diode and a transistor, though modern buck converters often use a second transistor instead of a diode for synchronous rectification) and at least one energy storage element, such as capacitance, inductance, or a combination of the two.

Filters consisting of capacitors (often paired with inductors) are typically added to the output (load-side filter) and input (power-side filter) of this type of converter to reduce voltage ripple.

As DC-DC converters, switching converters (such as step-down converters) are more efficient than linear regulators. Linear regulators are less complicated circuits that reduce voltage by dissipating energy as heat. However, the output current will not be increased. Buck converters are extremely efficient (often greater than 90%), making them ideal for converting the computer's primary (large-capacity) power supply voltage (about 12 V) to the lower voltages required by USB, DRAM, and the CPU (5V, 3.3V or 1.8V).

One of the most often used DC-DC converters is the step-down DC-DC converter, also known as Buck converter. The buck converter may reduce a greater DC voltage to a lower DC value, such

as from 24V to 12V or 5V. The buck converter offers a wide range of applications, low losses, and great efficiency.

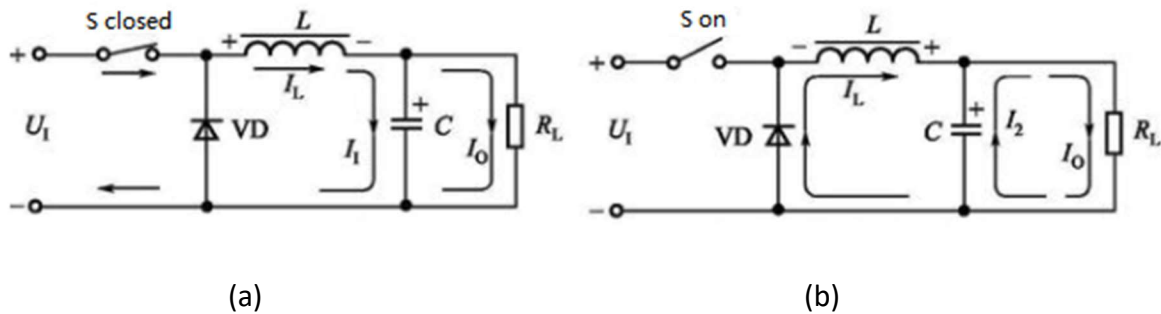


Fig: - 11 (a) Current path when  $V_T$  is on, (b) Current path when  $V_T$  is off

**Operating Principle :** In the tube that controls the power switch under the control of the pulse width modulation (PWM) signal, the  $V_T$  of the step-down DC/DC converter is switched on and off (also called cut-off) alternately. PWM is analogous to a mechanical switch that closes and opens at a fast speed. Figure 11 depicts its functioning principle. Figures 11(a) and 11(b) depict the current path when  $V_T$  is turned on and off, respectively. To make circuit analysis easier, the figure replaces the turning on and off of  $V_T$  by the shutting and opening of switch  $S$ . When  $V_T$  is activated (i.e.,  $S$  is closed), the freewheeling diode  $V_D$  is disabled, and the input voltage  $U_1$  is applied to the left end of the energy storage inductor  $L$ , resulting in a voltage of  $(U_1 - U_0)$ . The energy stored in the inductor increases linearly as the current  $I_L$  running through  $L$  increases. The inductor's induced electromotive force is left "+" and right "-." During this time, the input current (i.e., the inductor current  $I_L$ ) charges the filter capacitor  $C$  in addition to giving power to the load. The sum of the capacitor charging current  $I_1$  and the load  $R_L$  current  $I_0$  is the inductor current  $I_L$ .

The inductor  $L$  is detached from  $U_1$  when  $V_T$  is switched off (i.e.  $S$  is unplugged), as indicated in Figure 11(a). Because the current in the inductor cannot fluctuate abruptly, an induced voltage of left "-" and right "+" is generated on  $L$  to keep the current  $I_L$  through the inductor constant. The freewheeling diode  $V_D$  is turned on at this point, converting the magnetic field energy stored in  $L$  into electric energy, which continues to give power to the load through the loop formed by  $V_D$ , while the inductor current  $I_L$  declines linearly. At this point, the filter capacitor  $C$ 's



discharge current  $I_2$  is superimposed over the inductor current  $I_L$  to deliver power to the load  $R_L$ . The total of the inductor current  $I_L$  and the capacitor discharge current  $I_2$  is the load current  $I_O$ .

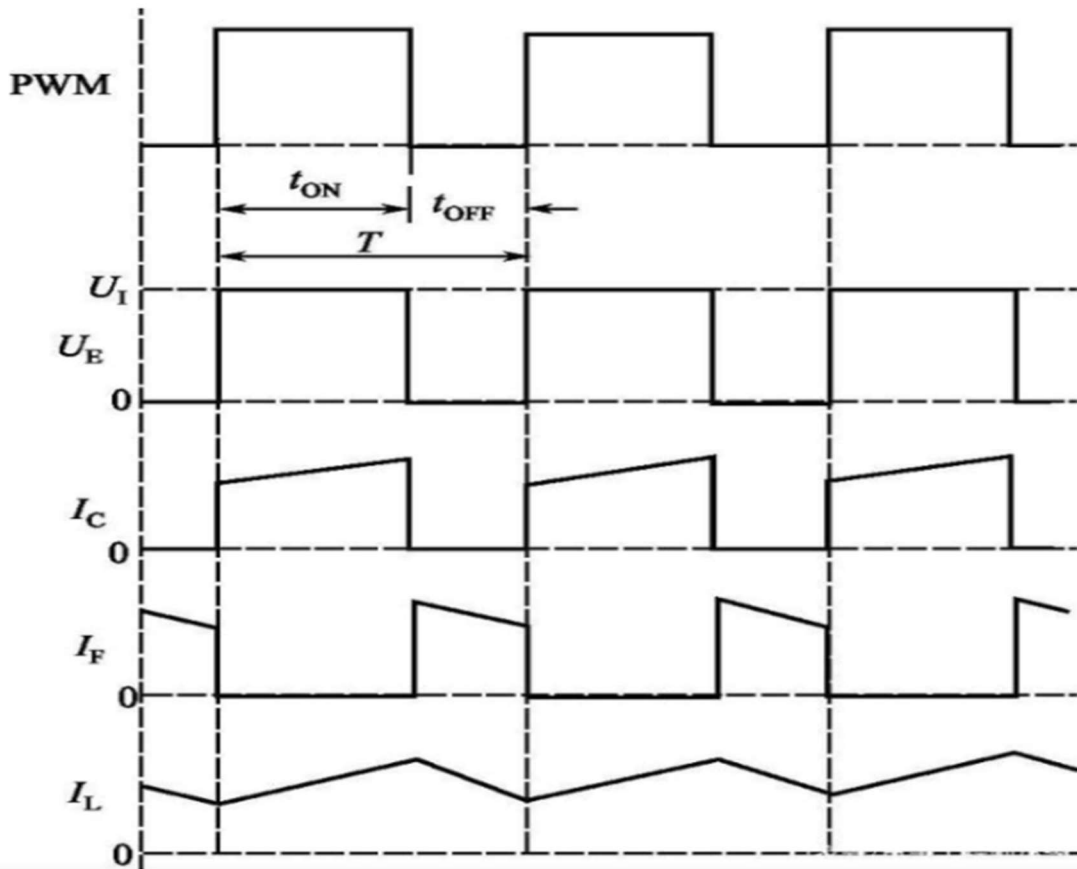


Fig 12: - Voltage and current waveforms of a DC/DC Buck converter

Figure 12 depicts the voltage and current waveforms of a step-down DC-DC converter. PWM is the pulse width modulation waveform,  $t_{ON}$  is the power switch  $V_T$ 's on time, and  $t_{OFF}$  is the power switch  $V_T$ 's off time. The switching time,  $T$ , is equal to the sum of  $t_{ON}$  and  $t_{OFF}$ , or  $T = t_{ON} + t_{OFF}$ . The duty cycle is the ratio of  $t_{ON}$  to  $T$ , which is denoted by the letter "D," as in  $D = t_{ON}/T$ .

The power switch tube  $V_T$ 's emitter voltage waveform is  $U_E$ , and the collector current waveform is  $I_C$ . The current waveform of the freewheeling diode  $V_D$  is represented by  $I_F$ . The filter inductor's current waveform is  $I_L$ . When the power switch tube  $V_T$  is turned on, the emitter voltage  $U_E$  equals the input voltage  $U_I$ , and when  $V_T$  is turned off, the emitter voltage  $U_E$  is zero. The inductor current increases linearly during the  $V_T$  on-time of the power switch and falls

linearly during the  $V_T$  off-time. The collector current  $I_C$  of  $V_T$  and the current  $I_F$  of the freewheeling diode  $V_D$  combine to create the inductor current  $I_L$ .

The average value of the filter inductor current  $I_L$  equals the DC-DC converters output current  $I_O$ . The inductor ripple current is the difference between the peak and valley values in the inductor current waveform. To reduce output current ripple,  $L$  should be large enough to allow the DC-DC converter to operate in continuous mode. The ripple current should typically be around 20% of the rated output current.

Now here in this topology under the concern of project (figure 15), when the circuit operates in the buck mode, the voltage-doubling rectifier circuit consisting of switch  $S_3$  and  $S_4$  becomes a voltage lowering inverter circuit. The power flows into the reduced voltage inverter circuit to get an AC power wave with an amplitude lower than  $V_H$ , and then passes through the transformer-isolated LC-LC resonant circuit and the rectifier circuit composed of the switch  $S_1$  and  $S_2$ . In Buck mode, the main inductor  $L$  and energy storage capacitor  $C_L$  (Parallel Low voltage element) form an LC filter, which filters out the high frequency components (i.e. acts as low-pass filter) in the circuit to obtain a better ripple free DC component to store the energy in the low voltage side.

In the boost mode and the buck mode, the switching MOSFETs in the circuit can realize *ZVS on*. At the same time, the freewheeling diode (along with the body diode of MOSFETs) in the circuit can realize *ZCS-off*. The soft switching state greatly improves the working efficiency of this converter, reducing the parasitic fashioned switching losses.

In the DC-DC Converter, isolation is necessary due to practical limitations of the semiconductor components are used in this system. Not only they are sensitive to the ratings, but also they may perform some detrimental functions due to harmonic components, which is the inherent drawback power electronics world.

**(ii) SPWM Inverter:** - Before starting the discussion on SPWM Inverter working procedure, it is quite necessary to understand the functionality of *PWM* Pulse Generating component of Inverter circuit.

The SPWM technique is carried out by using two types of waveform, one is reference waveform which is going to be modulated and the other is carrier waveform. The reference waveform is the sinusoidal waveform with fundamental frequency and the carrier waveform is a triangular waveform with high frequency. The frequency of the carrier waveform *determines the switching frequency of the inverter*. With the increase in frequency of the carrier wave, switching frequency also increases. On the other hand, the frequency of the reference waveform *determines the inverter output frequency*. The output frequency is generated in terms of *compared output of carrier waveform and the reference waveform*. The fundamental frequency component of output voltage can be controlled by the modulation index.

$$\text{Modulation Index, } \mathbf{M} = (\text{Amplitude of Modulating Wave} / \text{Amplitude of carrier wave}) = \mathbf{A_m/A_{cr}} \quad \dots\dots\dots (1)$$

Where  $A_m$  and  $A_{cr}$  are the peak value of modulating waveform and carrier waveform. The modulation index is controlled by the peak amplitude, then in turns control the r.m.s output voltage of the inverter.

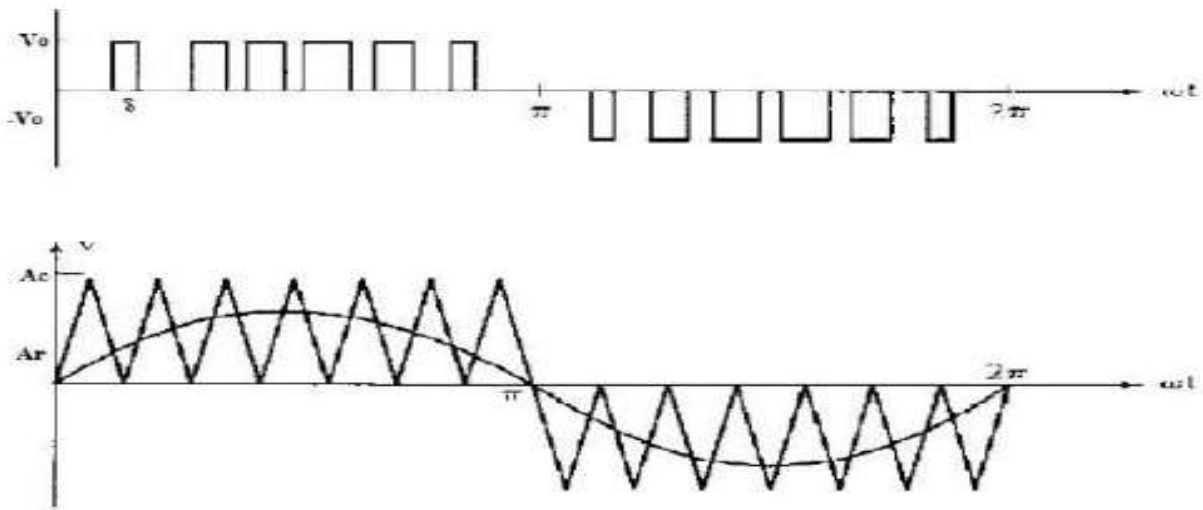


*Fig: -13 Sinusoidal Pulse Width Modulation*

The three phase inverters (figure 16) are generally used for high power applications like AC motor drives, induction heating, UPS devices etc. The 3 single phase half bridge inverters are connected in parallel to form a 3 phase voltage source inverter. A fixed DC voltage has given to

the inverter as input and has three phase-legs, each comprising MOSFET switches (Other switches can be used like IGBT, GTO etc.) combined with body diode, and a controlled AC output voltage is obtained by adjusting the ON-OFF periods of the inverter devices. The switches are opened and closed periodically in the proper sequence to get the desired output waveform. In the SPWM control, the switches of the inverter are controlled/triggered by comparison of a sinusoidal modulating signal with triangular carrier signal. The frequency ratio of the triangular carrier signal to the sinusoidal modulating signal is referred to as the modulation frequency ratio.

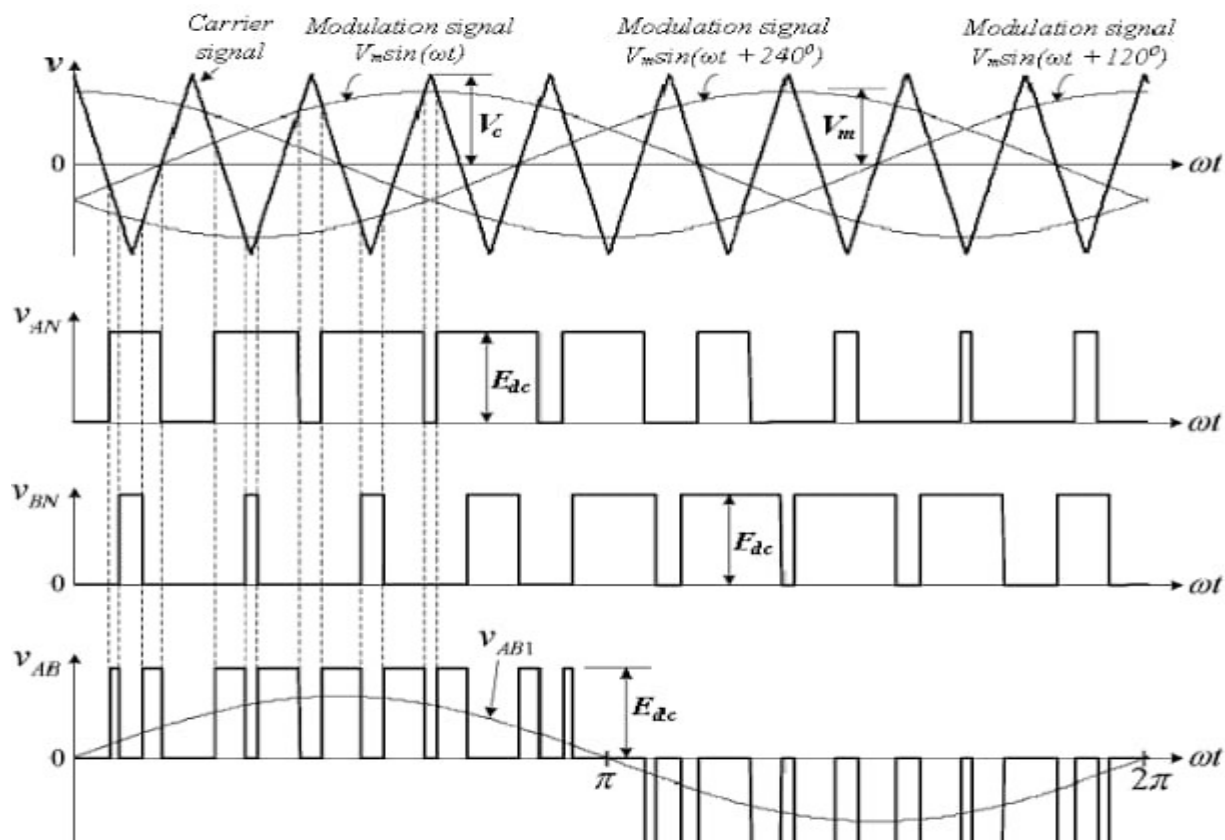


Fig: -14 Three Phase Sine-wave Pulse Width Modulation Waveform

In this method of modulation, several pulses per half-cycle is used. But instead of maintaining the width of the all pulses, the width of the each pulse is varied proportional with amplitude of a sine-wave evaluated at the centre of same pulse. The number of pulses per half cycle ( $N_p$ ) depends on the carrier frequency. Within the constraint that any two switches at anyone same

leg cannot conduct or operate at the same instant, the instantaneous output voltage can be shown by figure.

By adjusting the modulation index, the RMS output voltage can be varied. It can be observed that the area of each pulse corresponds approximately to the area under the sine-wave between the adjacent mid-points of OFF periods on the gating signals. If  $P_m$  is width of the  $m^{\text{th}}$  pulse then,

$$\text{RMS voltage, } E_L = E_{dc} \left( \sum_{m=1}^{N_p} P_m / \pi \right) \dots\dots\dots (2)$$

(i) For modulation index less than one, the largest harmonic amplitudes in the output voltage are associated with harmonics of order  $f_c/f_r \pm 1$  or  $(2N_p + 1)$ . Thus by increasing the number of pulses per half-cycle, the order of dominant harmonic frequency can be raised, which can then be filtered out easily. (ii) For modulation index greater than one, lower order harmonics appear since for modulation index greater than one, pulse width is no longer a sinusoidal function of the angular position of the pulse.

Basically there are two possible schemes for gating the devices. In one scheme, each switch can operate for  $180^\circ$  and for other scheme, they can conduct for  $120^\circ$ . In both the schemes, gating signals are and removed at  $60^\circ$  intervals of the output voltage waveform. Here in this topology, we employed the  $180^\circ$  conduction mode.

# **Chapter 4**

## **(Circuit Diagram)**

▪ **Circuit Diagram**

**(i) Bidirectional DC-DC Soft Switching Converter:**

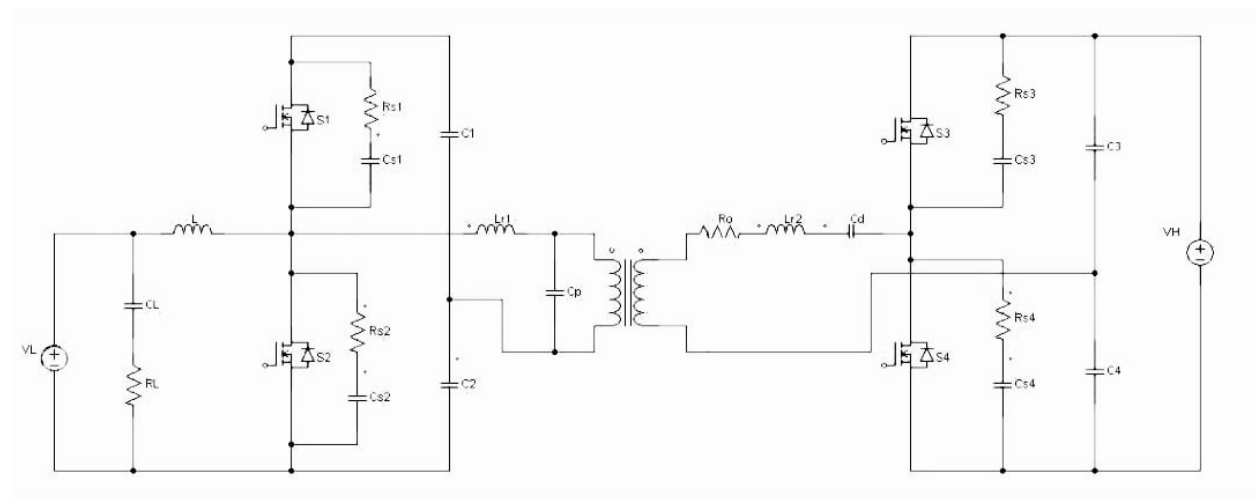


*Fig 15: - Schematic diagram of Bidirectional isolated DC-DC Converter*

**(ii) Three Phase DC-AC Converter:**

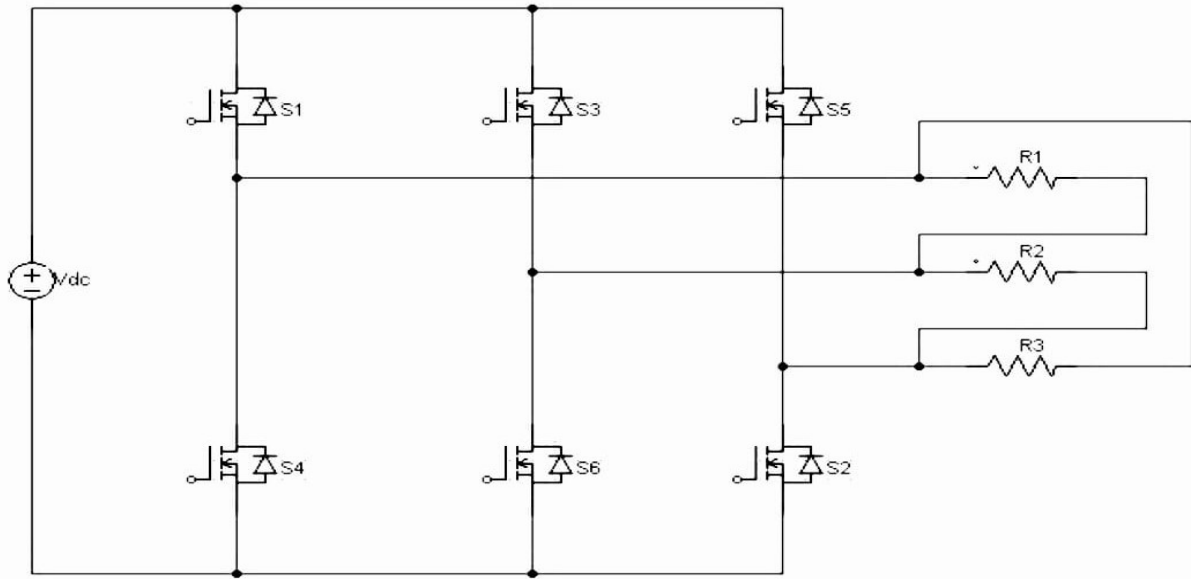


Fig 16: - Schematic diagram of Bidirectional isolated DC-DC Converter



# **Chapter 5**

**(Mathematical Modelling)**

➤ **DC to DC Converter:**

(i) **Boost Mode:** The operation under Boost Mode is divided into several stages by means different time domains like following;

Stage 1 ( $t_0 < t < t_1$ ): Stage 1 starts when the switch  $S_1$  is turned off. In Stage 1, both switches  $S_1$  and  $S_2$  are off. The resonant inductor  $L_{r1}$  is discharged and the inductor current decreases. The main inductor  $L$  is charged and the main inductor current  $i_L$  increases in a positive direction. The resonant capacitor  $C_{S1}$  is discharged and the resonant capacitor  $C_{S2}$  is charged. Power is transferred to load by capacitors  $C_3$  and  $C_4$ . The resonant inductor  $L_{r2}$  is charged through the diode  $D_{S4}$  and the inductor current direction is negative. When the capacitor  $C_{S1}$  is discharged completely and the capacitor  $C_{S2}$  is charged completely.

So, the voltage across the switch  $S_2$  is given by  $V_{S2}(t_2) = V_L / (1-D)$ ; .....(3)

Where  $D = \text{Duty Cycle}$

Stage 2 ( $t_1 < t < t_2$ ): At  $t = t_1$ , the main inductor  $L$  is charged. The antiparallel diode  $D_{S1}$  is turned on, and the voltage across  $S_1$  is clamped to 0, so the ZVS condition of  $S_1$  can be satisfied. At  $t = t_2$ , the switch  $S_1$  drive signal arrives, and mode 2 ends. Final values are  $i_{S1}=0$ ,  $i_{S2}=0$ ,  $V_{S1}=0$ ,  $V_{S2}=V_L/(1-D)$ .

The current flowing through the diode  $D_{S1}$  is given by,  $i_{D_{S1}}(t_2) = i_L(t_2) - i_{L_{r1}}(t_2)$  .....(4)

Stage 3 ( $t_2 < t < t_3$ ): At  $t = t_2$  switch  $S_1$  is turned on with ZVS. The main inductor  $L$  current begin to decrease linearly. The resonant inductor  $L_{r1}$  is charged through the capacitor  $C_1$ , the resonant capacitor  $C_p$ , and the switch  $S_1$ . The resonant inductor  $L_{r1}$  has a positive current. When the current of the resonant inductor  $L_{r2}$  decrease to zero. The diode  $D_{S4}$  is turned off with zero current.

The equation of various currents for this mode is given by,

$$i_L(t) = I_L(t_2) - (t-t_2) \cdot [V_L - V_{C1}(t_2) - V_{C2}(t_2)]/L \quad \text{.....(5)}$$

$$i_L(t) = [V_{C1}(t_2) - V_{Cp}(t_2) / Z_r] \cdot \sin \omega_r (t-t_2) \quad \text{.....(6)}$$

$$i_{s1}(t) = i_{Lr1}(t) - i_L(t) \quad \text{.....(7)}$$

Where, Resonant Impedance,  $Z_r = [L_{r1}(C_1 + C_p)/C_1C_p]^{0.5}$  .....(8)

Resonant frequency,  $\omega_r = [(C_1+C_p)/L_{r1}C_1C_p]^{0.5}$  .....(9)

Stage 4 ( $t_3 < t < t_4$ ): In stage 4, the antiparallel diode  $D_{S3}$ ,  $D_{S4}$  are turned off and power is transferred to load by capacitors  $C_3$  and  $C_4$ . At  $t = t_4$ ,  $S_1$  is turned off. The voltage across antiparallel diodes  $D_{S3}$  and  $D_{S4}$  is 0, and the voltage across switch  $V_{S2} = V_L / (1-D)$ .

Stage 5 ( $t_4 < t < t_5$ ): In this stage, the switch  $S_1$  and  $S_2$  are both turned off. The voltage across the antiparallel diode  $D_{S3}$  decreases to 0. The resonant inductor  $L_{r2}$  current increases in a positive direction. The resonant capacitor  $C_{S1}$  is charged and the resonant capacitor  $C_{S2}$  is discharged. At  $t = t_5$ ,  $C_{S2}$  is discharged completely, and  $C_{S1}$  is charged to  $V_L / (1-D)$ .

Stage 6 ( $t_5 < t < t_6$ ): At  $t = t_5$ , antiparallel diode  $D_{S2}$  is turned on, resonant inductor  $L_{r1}$  is discharged through capacitor  $C_2$  and diode  $D_{S2}$ . The current in inductor  $L_{r1}$  continues to decrease, and the current of main inductor  $L$  also decreases. Since  $D_{S2}$  is turned on, the voltage across the switch  $S_2$  is clamped to 0, so  $S_2$  can be turned on with ZVS condition. The diode  $D_{S3}$  is still on and the current in the inductor  $L_{r2}$  continues to change in the positive direction. When the switch  $S_2$  drive signal arrives, stage 7 ends.

Voltage across Switch  $S_1$ ;  $V_{s1}(t_6) = V_L / (1-D)$ ; .....(10)

Current through  $D_{S2}$ ;  $i_{DS2}(t_6) = i_L(t_6) - i_{Lr1}(t_6)$ ; .....(11)

Stage 7 ( $t_6 < t < t_7$ ): At  $t = t_6$  switch  $S_2$  is turned on with ZVS. The main inductor  $L$  starts charging linearly. Inductor  $L_{r1}$ , capacitor  $C_2$  and  $C_p$  resonant with each other. The antiparallel diode  $D_{S3}$  is in on state, the current in the resonant inductor  $L_{r2}$  continues to maintain a positive change. When the current in the resonant inductor  $L_{r2}$  decrease to 0, the diode  $D_{S3}$  turns off with zero current.

The equation of various currents for this interval is:

$$i_L(t) = i_L(t_6) - (t-t_6) \cdot [V_L] / L \quad \text{.....(12)}$$

$$i_L(t) = [V_{c2}(t_6) - V_{Cp}(t_6) / Z_r] \cdot \sin \omega_r (t-t_6) \quad \text{.....(13)}$$

$$i_{s2}(t) = i_{Lr2}(t) - i_L(t) \quad \text{.....(14)}$$

Where, Resonant Impedance,  $Z_r = [L_{r1}(C_2 + C_p)/C_2C_p]^{0.5}$  .....(15)

Resonant frequency,  $\omega_r = [(C_2+C_p)/L_{r1}C_2C_p]^{0.5}$  .....(16)

Stage 8 (t7<t<t8): In this stage, the antiparallel diodes  $D_{S3}$ ,  $D_{S4}$  are both turned off and power to load is transferred by output capacitor  $C_3$  and  $C_4$ . When the switch  $S_2$  is turned off, mode 8 ends.

**(ii) Buck Mode:** In buck mode, the voltage-doubling rectifier circuit composed of switch  $S_3$  and  $S_4$  becomes a half-voltage inverter circuit. The circuit operating mode is a little different from the boost mode, but the overall operating principle is similar.

➤ **DC-AC Converter in 180° Conduction Mode:**

In this conduction mode, each device will be in conduction with 180° where they are activated at intervals with 60°. The output terminals like A, B, and C are connected to the star or 3 phase delta connection of the load. That means whether the load is Star or Delta connected, the mathematical principle will be equal in both case. In this project, we took the delta load but the following set of equations are for Star Load.

**(i) During Interval I for  $0 \leq \omega t \leq 60^\circ$**

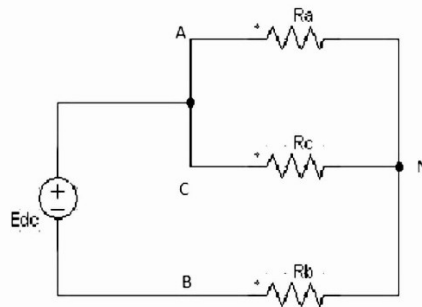


Fig: - 17 Equivalent Circuit at Interval I

Equivalent Resistance,  $R_{eq} = R + R/2 = 3R/2$  (as  $R_a = R_b = R_c = R$ ) .....(17)

Current  $I_1 = E_{dc} / R_{eq} = 2E_{dc}/R_{eq}$  .....(18)

Now,  $E_{AN} = E_{CN} = I_1.R/2 = E_{dc}/3$  .....(19)

Also,  $E_{BN} = - I_1.R = - 2E_{dc}/3$  .....(20)

(ii) During Interval II for  $60^\circ \leq \omega t \leq 120^\circ$

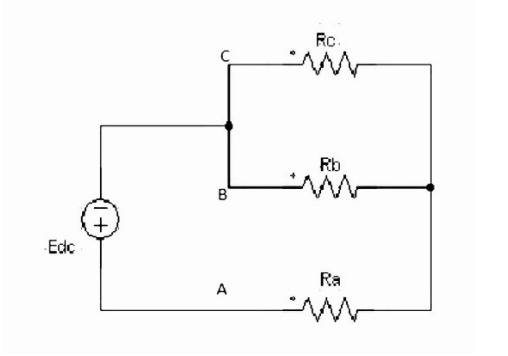


Fig: - 18 Equivalent Circuit at Interval II

Equivalent Resistance,  $R_{eq} = R + R/2 = 3R/2$  .....(21)

Current  $I_2 = E_{dc} / R_{eq} = 2E_{dc}/R_{eq}$  .....(22)

Now,  $E_{AN} = I_2.R = 2E_{dc}/3$  .....(23)

$E_{BN} = E_{CN} = - I_2.R/2 = - E_{dc}/3$  .....(24)

(i) During Interval III for  $120^\circ \leq \omega t \leq 180^\circ$

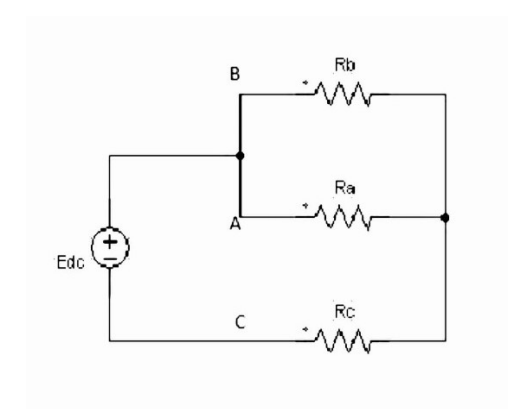


Fig:- 19 Equivalent Circuit at Interval III

Equivalent Resistance,  $R_{eq} = R + R/2 = 3R/2$  .....(25)

Current  $I_3 = E_{dc} / R_{eq} = 2E_{dc}/R_{eq}$  .....(24)

Now,  $E_{AN} = E_{BN} = I_3 \cdot R/2 = E_{dc}/3$  .....(26)

Also,  $E_{CN} = - I_3 \cdot R = - 2E_{dc}/3$  .....(27)

The instantaneous line-to-line voltage  $E_{AB} = E_{AN} - E_{BN}$  can be expressed in terms of Fourier-series, recognizing that  $E_{AB}$  is shifted by  $30^\circ$  and even harmonics are zero.

$$E_{AB} = \sum_{n=1,3,5,\dots}^{\infty} (4E_{dc} / n\pi) \cos(n\pi/6) [\sin n(\omega t + \frac{\pi}{6})] \quad \text{.....(28)}$$

$E_{BC}$  and  $E_{CA}$  can also be found above equation by phase shifting  $E_{AB}$  by  $120^\circ$  and  $240^\circ$ , respectively.

$$E_{BC} = \sum_{n=1,3,5,\dots}^{\infty} (4E_{dc} / n\pi) \cos(n\pi/6) [\sin n(\omega t - \frac{\pi}{2})] \quad \text{.....(29)}$$

$$E_{CA} = \sum_{n=1,3,5,\dots}^{\infty} (4E_{dc} / n\pi) \cos(n\pi/6) [\sin n(\omega t - \frac{7\pi}{6})] \quad \text{.....(30)}$$

For  $n = 3, 9, 15 \dots$ ,  $\cos(n\pi/6) = 0$

The Line-to-line RMS Voltage can be found from the following equation,

$$E_L = \left[ \frac{2}{\pi} \int_0^{2\pi/3} E_{dc}^2 d(\omega t) \right]^{0.5} = (2/3)^{0.5} \cdot E_{dc} = 0.8165 E_{dc} \quad \text{.....(31)}$$

The RMS of nth Component of the line voltage is,

$$E_{Ln} = [4 E_{dc} / (1.414 \cdot n \cdot \pi)] \cos(n\pi/6) \quad \text{.....(32)}$$

For  $n = 1$ ;  $E_{L1} = [4 E_{dc} / (1.414 \cdot \pi)] \cos(30) = 0.7797 E_{dc}$  .....(33)

The RMS value of line-to-neutral voltages can be found from the line voltages,

$$E_p = E_L / 1.732 = 1.414 E_{dc} / 3 = 0.4714 E_{dc} \quad \text{.....(34)}$$

# **Chapter 6**

## **(Software Simulation)**

▪ **Software Simulation**

**(1) Overall block diagram of the entire system: -**

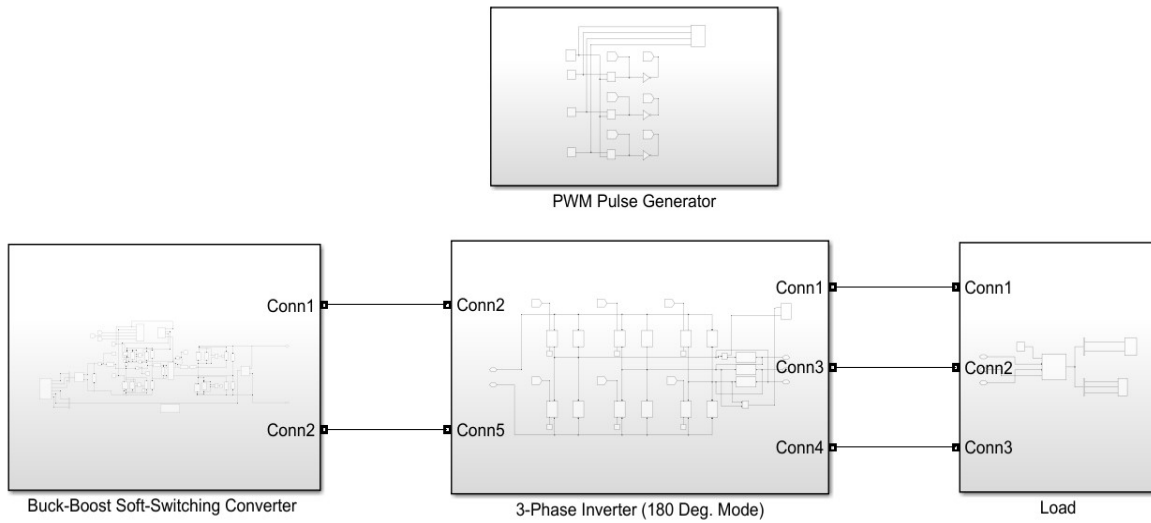


**Fig: - 20**

**(2) Buck-Boost Soft-switching converter: -**

**(A) Boost Mode**



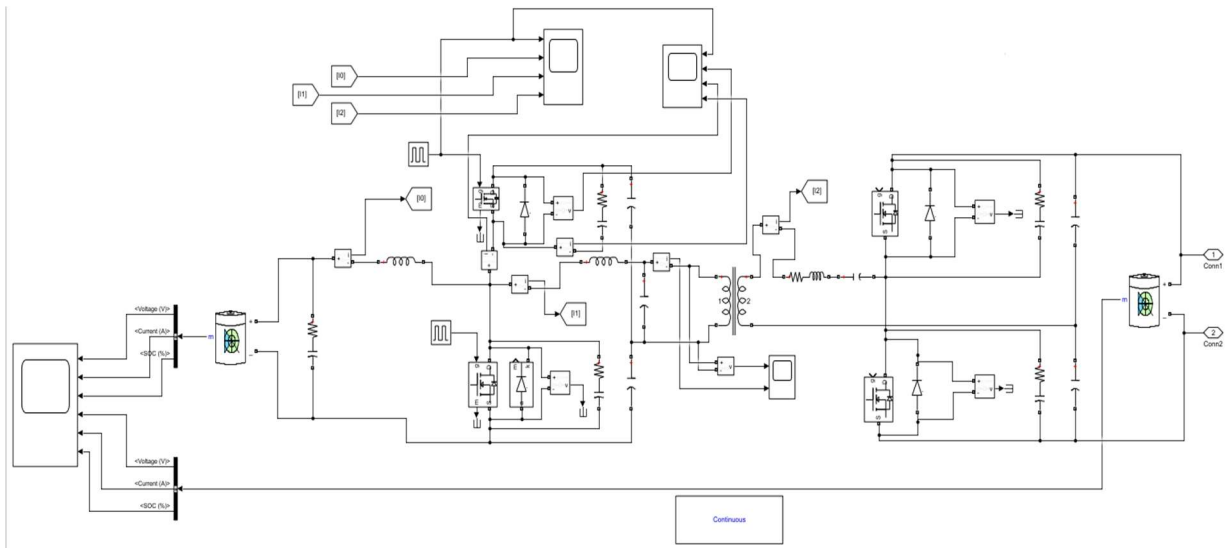


**Fig: - 21 Simulation diagram of DC-DC Soft-Switching Converter (Boost Mode)**

**(B) Buck Mode**

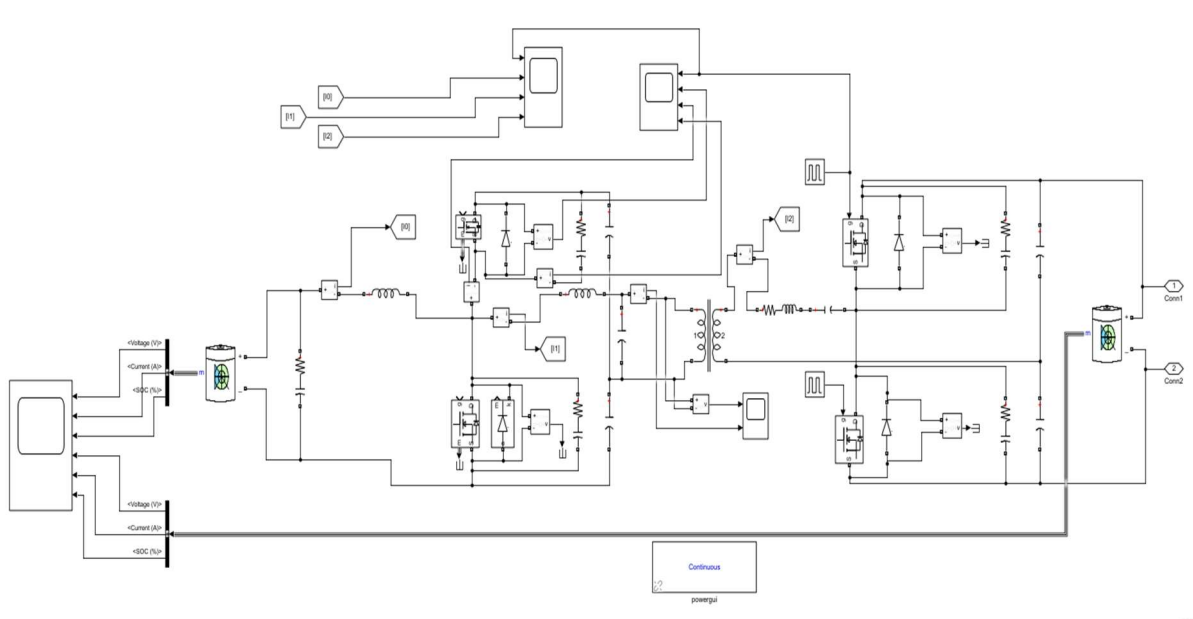


**Fig: -22 Simulation diagram of DC-DC Soft-Switching Converter (Buck Mode)**

**(3) DC-AC Converter (Inverter): -**

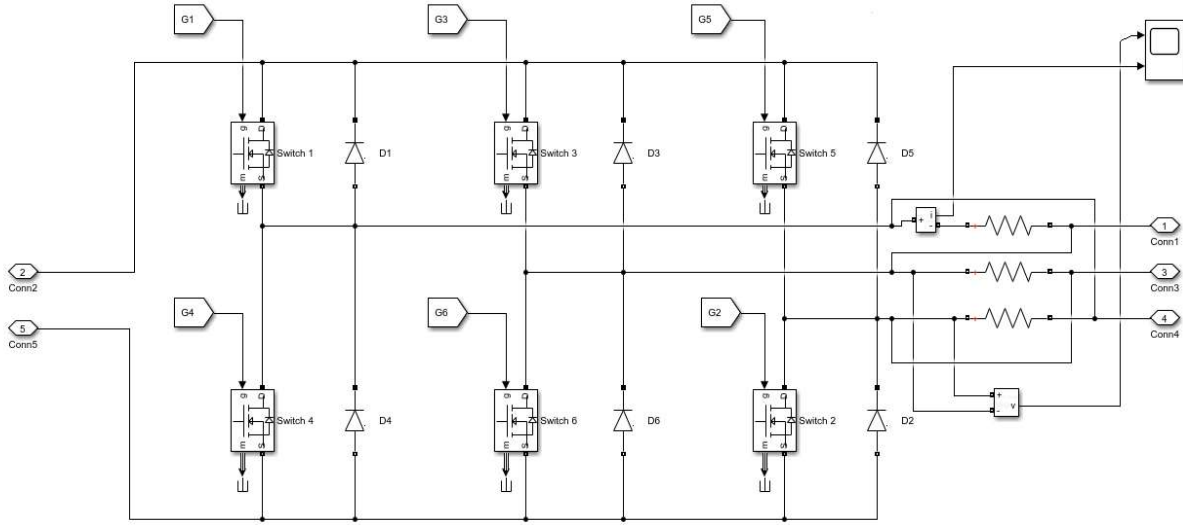


**Fig: - 23** Three Phase DC-AC Inverter with 180° conduction mode

**(4) Load: -**

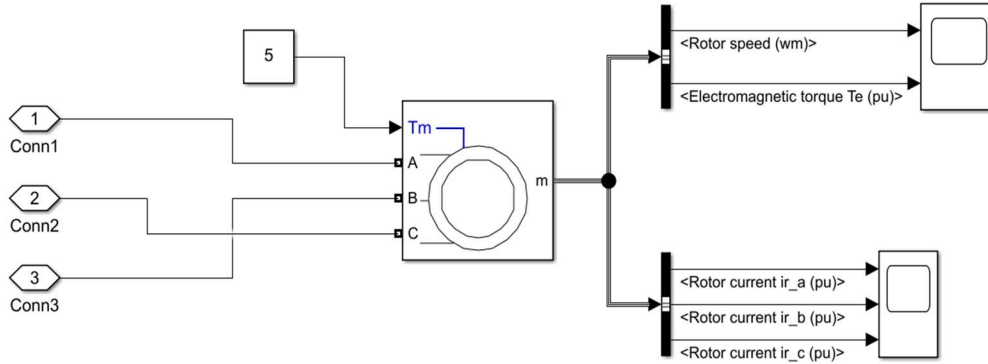


**Fig: - 24** Load with 3-phase Asynchronous Induction Motor

**(5) SPWM Pulse Generation Circuit: -**

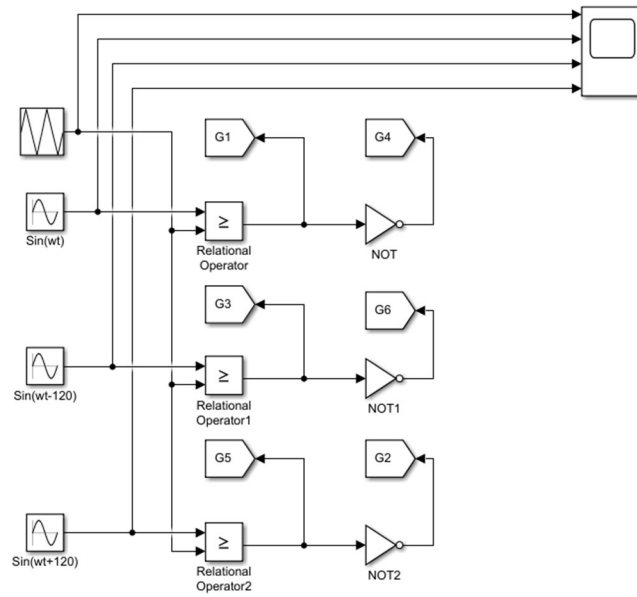


**Fig: - 25 SPWM Pulse Generator circuit with Sinusoidal triggering Input and Triangular Carrier Input**

# **Chapter 7**

## **(Observation and Results)**

■ **Observations and results**

**(1) Battery Parameters: (A) Boost Mode**

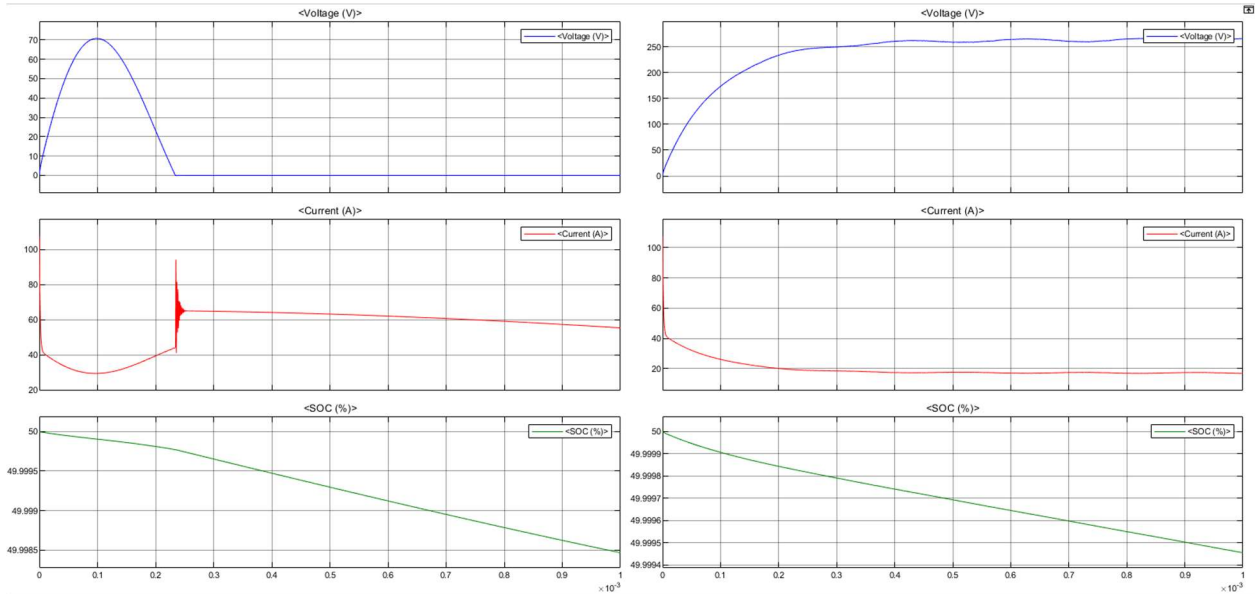


**Fig: - 26** (a) Voltage, Current & SOC of LV Battery (Left Column from top to Bottom); (b) Voltage, Current & SOC of HV Battery (Right Column from top to Bottom)

**(B) Buck Mode**

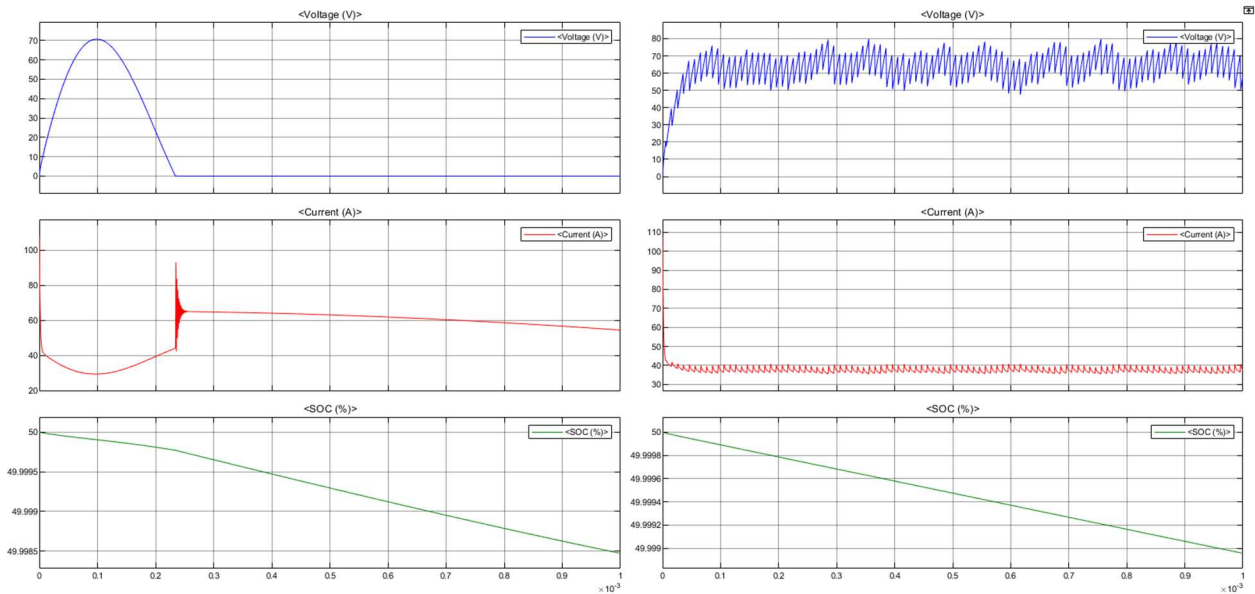


**Fig: - 27** (a) Voltage, Current & SOC of LV Battery (Left Column from top to Bottom); (b) Voltage, Current & SOC of HV Battery (Right Column from top to Bottom)

### (3) Boost Mode Switching and Inductor Parameters:

(A)

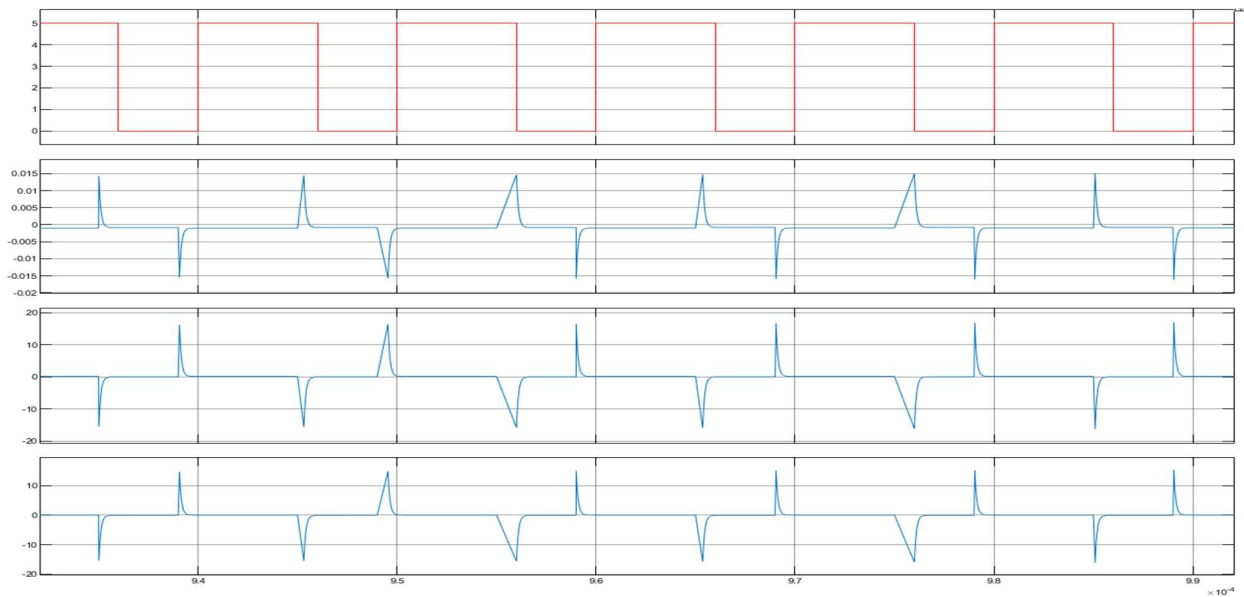


Fig: - 28 (a) Pulse Waveform; (b) Voltage across MOSFET, (c) Current through MOSFET, (d) Snubber Current

(B)

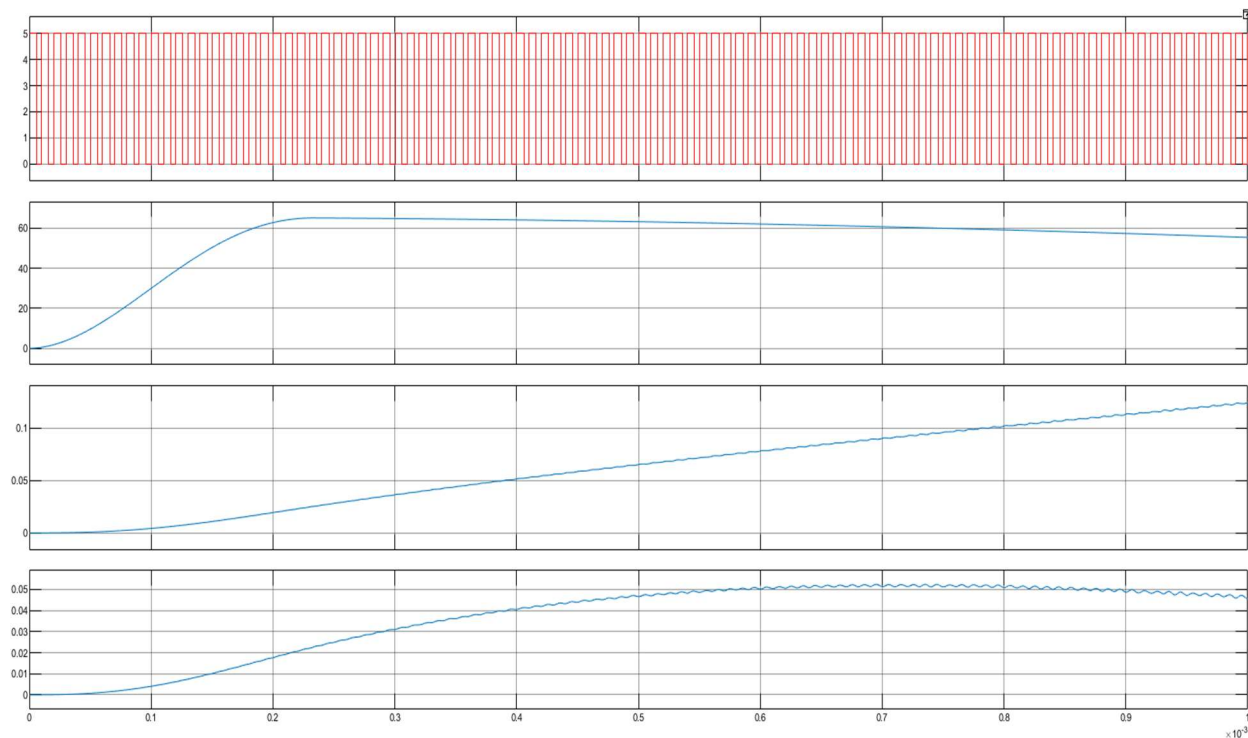
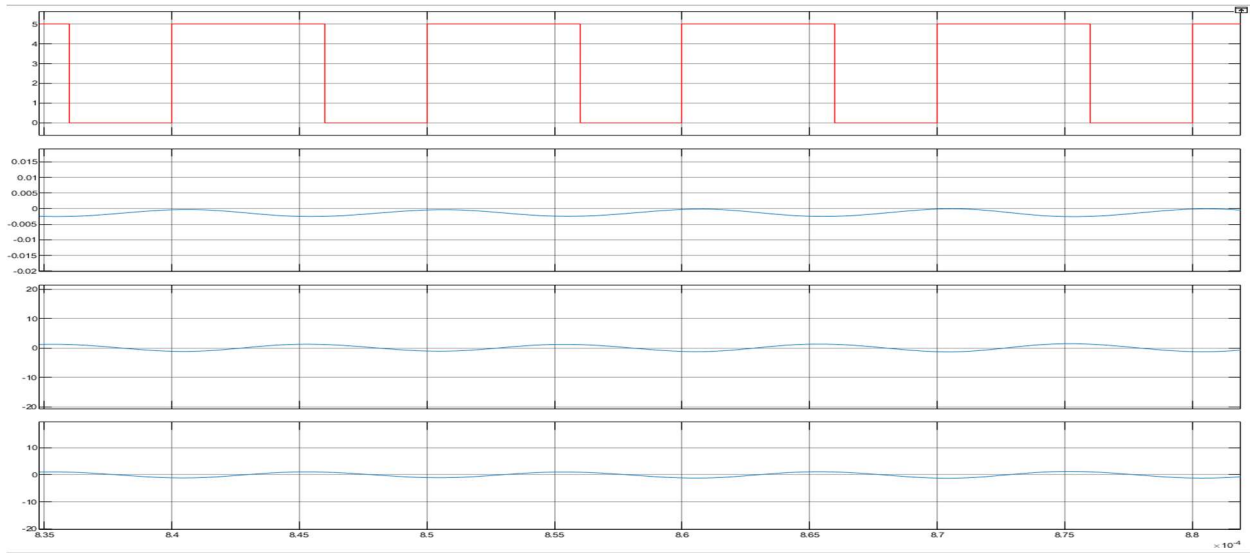


Fig: - 29 (a) Pulse Waveform, (b) Current of inductor L, (c) Current of Inductor  $L_{r1}$ , (d) Current through  $L_{r2}$

#### (4) Buck Mode Switching and Inductor Parameters:

(A)



**Fig: - 30** (a) Pulse Waveform; (b) Voltage across MOSFET, (c) Current through MOSFET, (d) Snubber Current

(B)

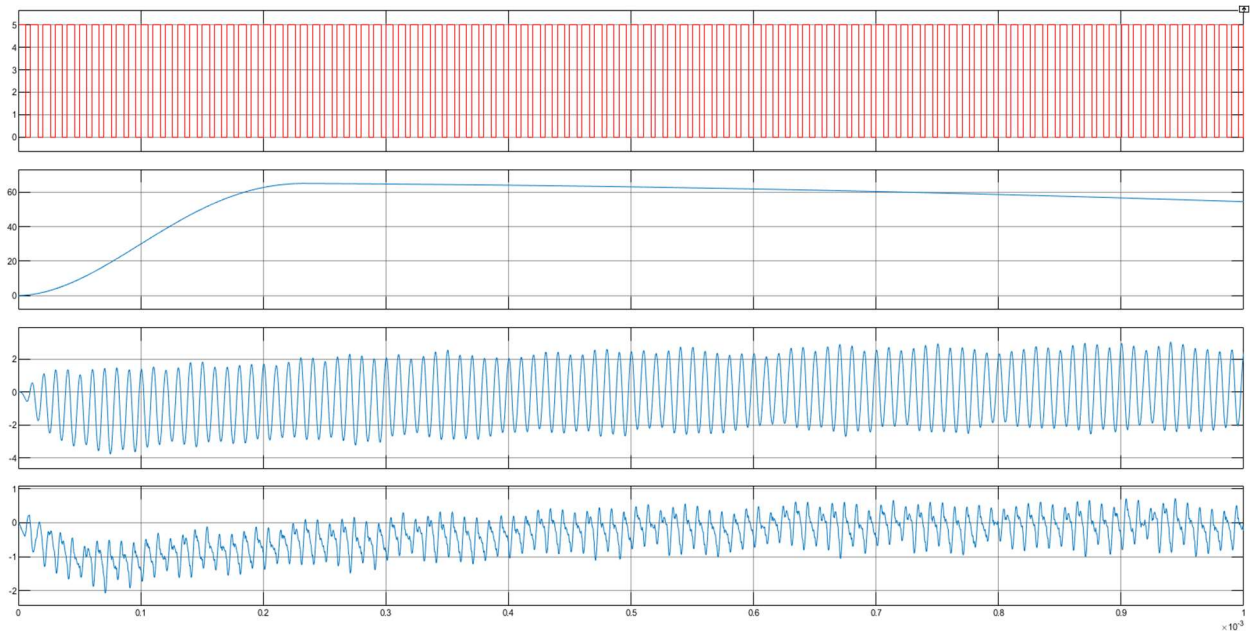


**Fig: - 31** (a) Pulse Waveform, (b) Current of inductor L, (c) Current of Inductor  $L_{r1}$ , (d) Current through  $L_{r2}$

**(5) Transformer parameters: (a) Boost Mode**

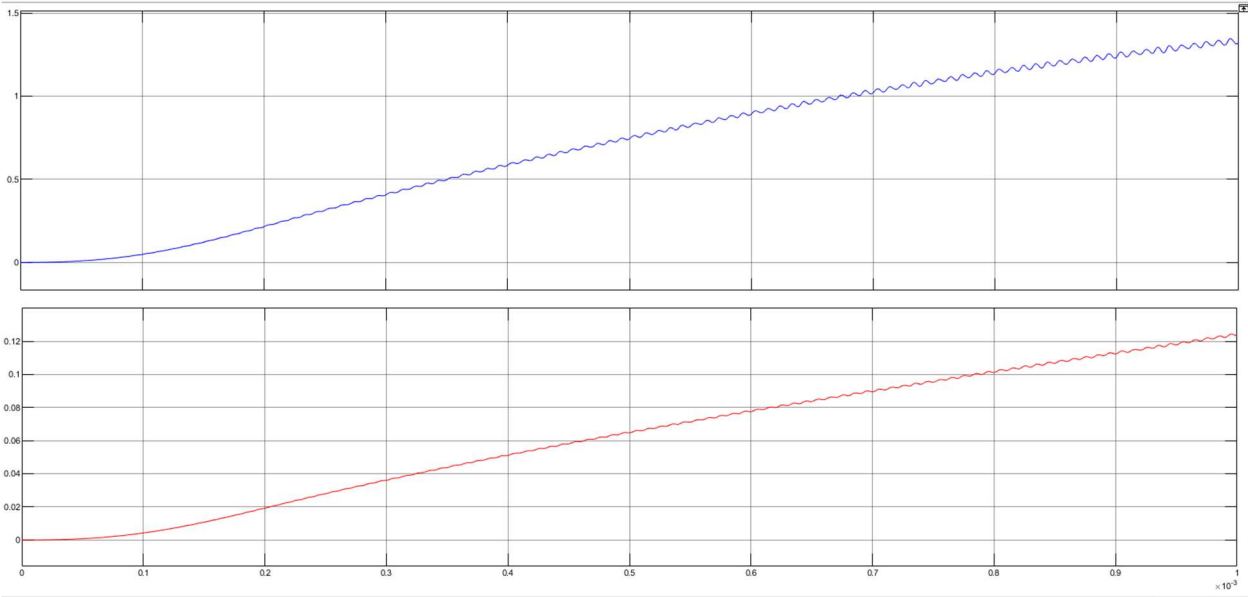


**Fig: - 32 (a) Transformer Voltage; (b) Transformer Current (From top to bottom) for Boost Mode**

**(b) Buck Mode**

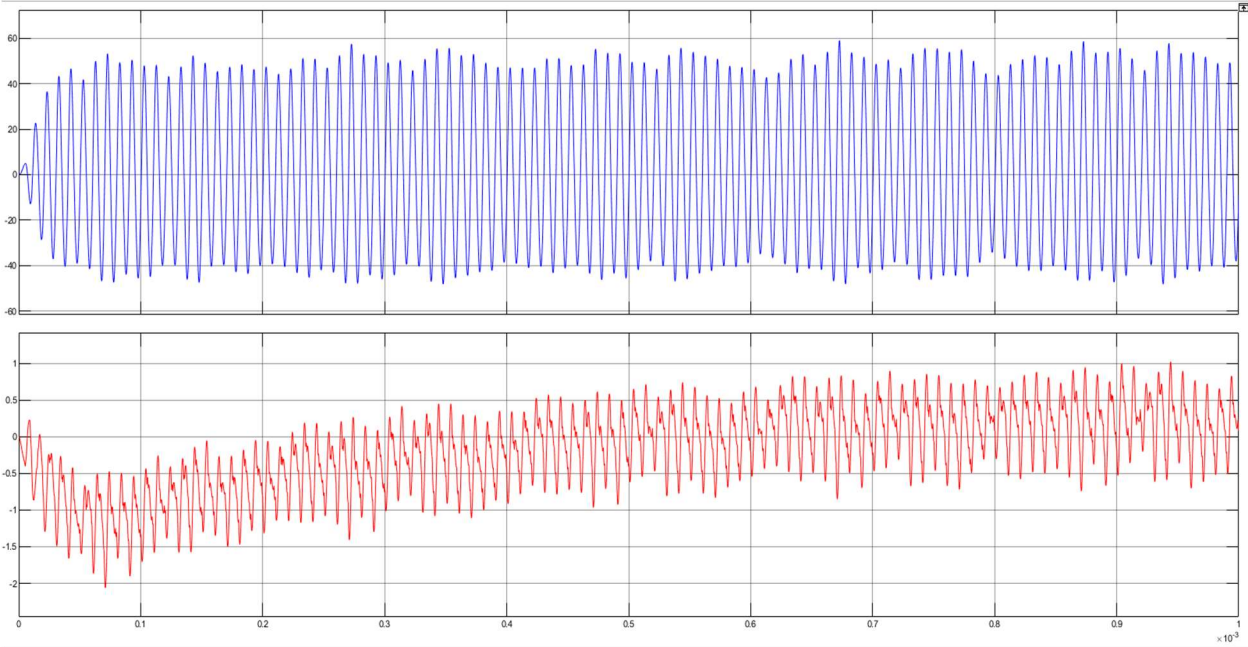


**Fig: - 33 (a) Transformer Voltage; (b) Transformer Current (From top to bottom) for Buck Mode**



### (6) Output graph at Inverter: (a) Buck Mode

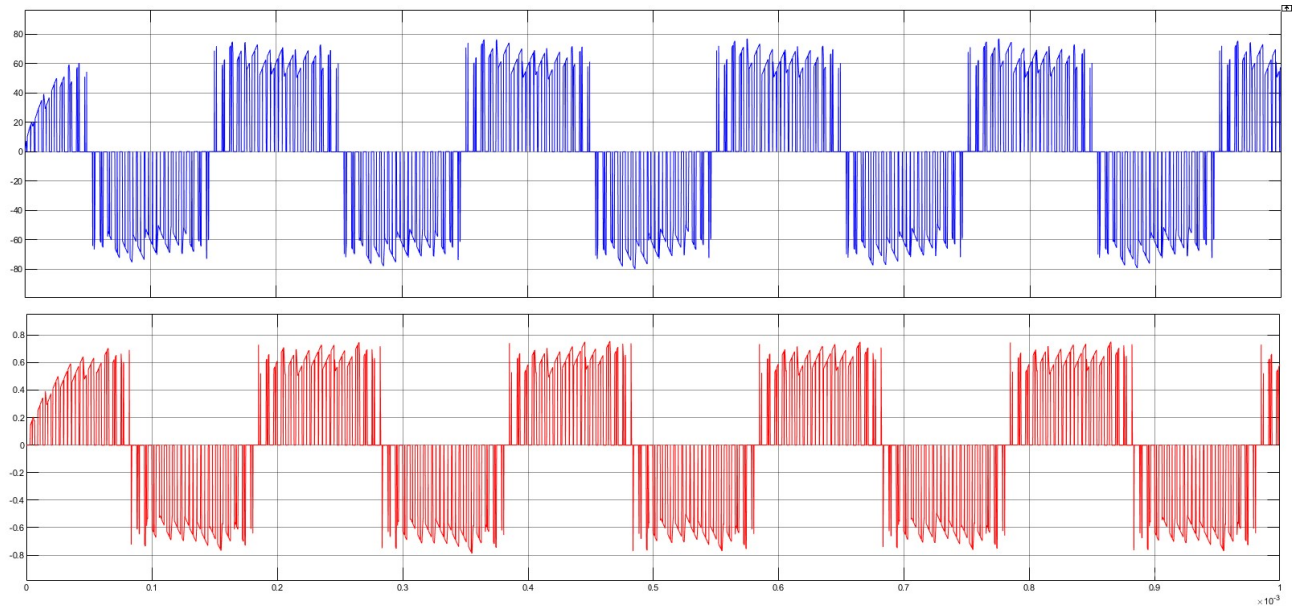


**Fig: - 34** (a) Inverter output Phase-to-Phase Voltage; (b) Inverter output Phase Current (From top to bottom) for Buck Mode

### (b) Boost Mode

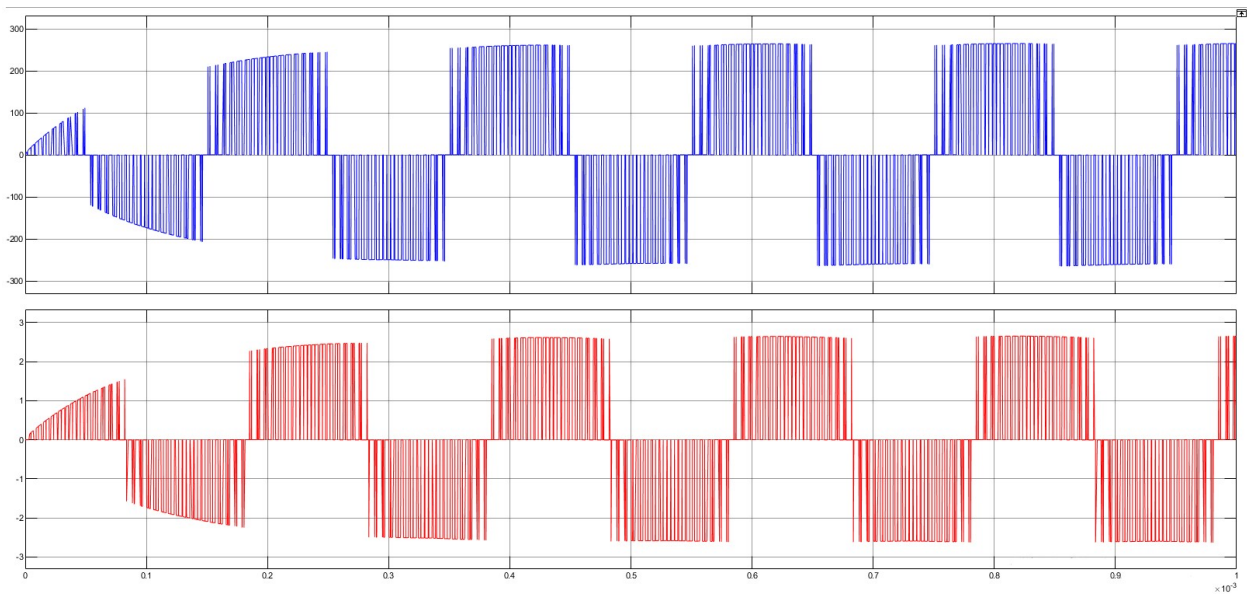


**Fig: - 35** (a) Inverter output Phase-to-Phase Voltage; (b) Inverter output Phase Current (From top to bottom) for Boost Mode

### (7) Output graph Load Section: (a) Buck Mode

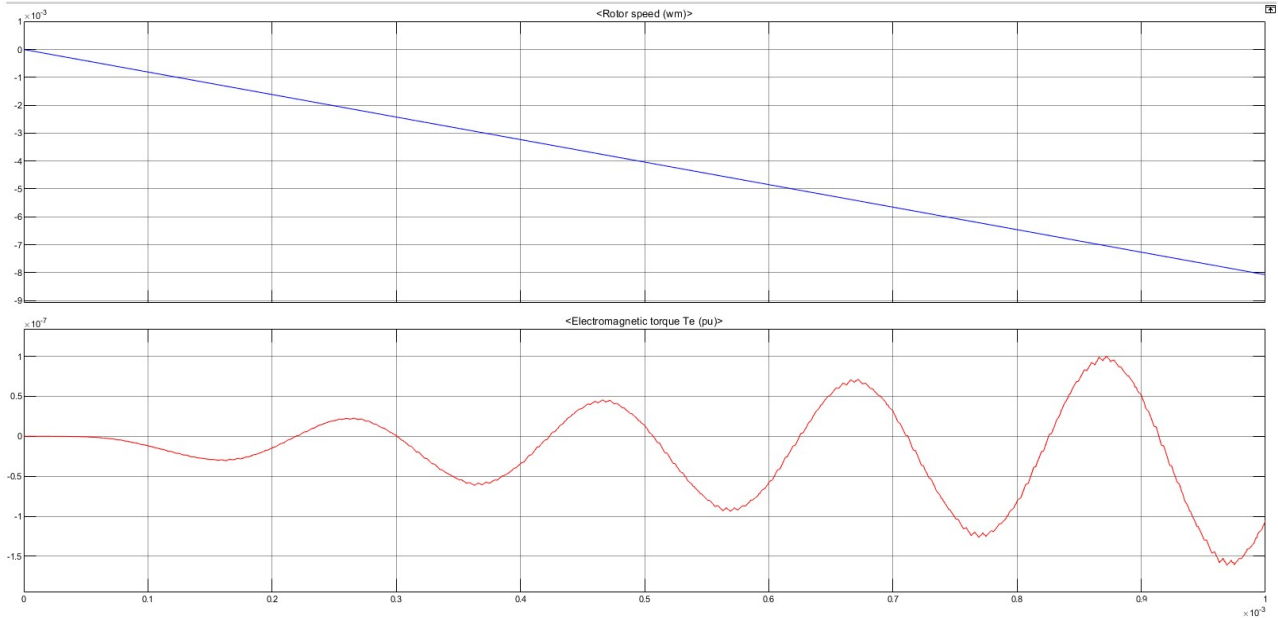


**Fig: -36** (a) Speed of Asynchronous Machine; (b) Torque of Asynchronous Machine (From top to bottom) for Buck Mode

### (b) Boost Mode

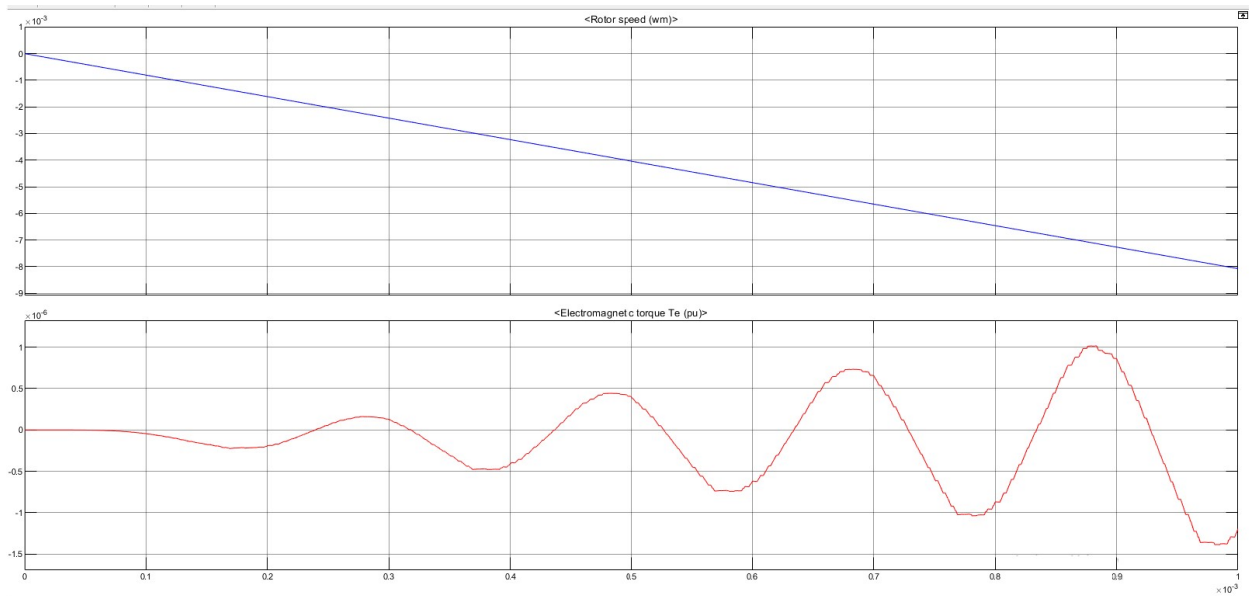


**Fig: -37** (a) Speed of Asynchronous Machine; (b) Torque of Asynchronous Machine (From top to bottom) for Boost Mode

**(7) SPWM Pulse triggering graph:**

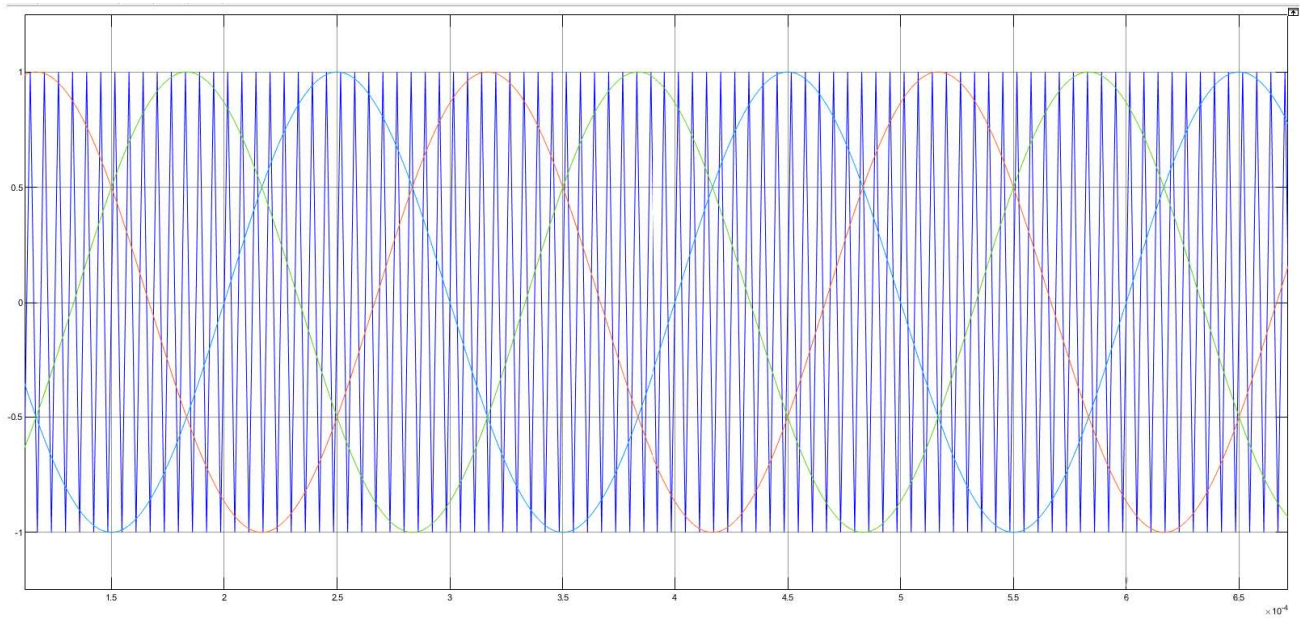


**Fig: - 38** Three-Phase SPWM Pulse Generation Curve

**(8) Outcome values of each parameter: - (A) Boost Mode**

<b><i>Parameter Names</i></b>	<b><i>Respected Values</i></b>
<b>A. Pulse Generation</b>	
Switching frequency	100 kHz
Pulse Amplitude	5 unit
Duty Cycle	60%-40%
<b>B. MOSFET</b>	
MOSFET Voltage	+ - 0.01 – 0.03 Volts
MOSFET Current	+ - 12-13 Amps
Snubber Current	+ - 10-11 Amps
<b>C. Transformer</b>	
Voltage	1.6 Volts
Current	0.121 Amps
<b>D. Inductor Current</b>	
Inductor Current 1	Nearly 60 Amps
Inductor Current 2	Nearly 0.12 Amps
Inductor Current 3	Nearly 0.05 Amps

<b>E. Inverter Output</b>	
Phase-to-Phase Voltage	+ - 250 Volts
Phase Current	+ - 2.5 Amps
<b>F. Load</b>	
Speed	$-8.5 \cdot 10^{-3}$ p.u.
Torque	$+ - 1 \cdot 10^{-3}$ p.u.

*Table: 1*

(B) Buck Mode

<i>Parameter Names</i>	<i>Respected Values</i>
<b>A. Pulse Generation</b>	
Switching frequency	100 kHz
Pulse Amplitude	5 unit
Duty Cycle	60%; 40%
<b>B. MOSFET</b>	
MOSFET Voltage	2 mV
MOSFET Current	+ - 1 .1 Amps
Snubber Current	+ - 1 Amps
<b>C. Transformer</b>	
Voltage	+ - 40-50 Volts
Current	+ - 0.5 Amps
<b>D. Inductor Current</b>	
Inductor Current 1	60 Amps
Inductor Current 2	+ - 2-2.5 Amps
Inductor Current 3	+ - 0.5-1 Amps
<b>E. Inverter Output</b>	
Phase-to-Phase Voltage	+ - 75 volts
Phase Current	+ - 0.72 Amps
<b>F. Load</b>	
Speed	$-0.85 \cdot 10^{-3}$ p.u.
Torque	$+ - 1 \cdot 10^{-6}$ p.u.

*Table: 2*

# **Chapter 8**

## **(Conclusion)**

## ▪ **Conclusion**

**1)** Soft-switching analysis and accurate modelling help the converter to achieve good circuit performance. The GSSA method was used to model and control the system. And a LCLC resonant bi-directional DC-DC converter with a power of 1000 W is built. The function of soft-switching is implemented. The experimental results are in good agreement with the theoretical results. The system efficiency is 95.56% in boost mode and 96.04% in buck mode.

**2)** Soft-switching techniques made possible the increasing demand of higher frequency converters with higher power density, high efficiency, compact size, and low EMI and losses. This article focus on various soft-switching techniques.

**3)** ZVS/ZCS reduces switching losses at turn-on and turn-off at the expense of high voltage/current stress. ZVT & ZCT provides soft-switching with minimum voltage/current stress on the main switch, perhaps these converters are faced with problems of limited voltage conversion range and variable frequency operation.

**4)** The passive components volume is reduced from 0.083 dm<sup>3</sup> to 0.010 dm<sup>3</sup> by varying the switching frequency from 50 kHz to 500 kHz. Thus, the overall volume of the converter is reduced with improved efficiency by considering higher switching frequency to the converter

# **Appendix A**

**(Specifications and Standard Values)**

▪ **Specification of Prototypes**

Specification/Parameter	Value
High-side Voltage	400 V
Low-side Voltage	200 V
Power rating	1 kW
Switching Frequency	100 kHz
Main inductance $L$	160 $\mu$ H
Resonant inductance $L_{r1} L_{r2}$	30 $\mu$ H
Resonant capacitance $C_p$	0.1 $\mu$ F
Auxiliary capacitor $C_d$	680 nF
Energy storage capacitor $C_L$	33 $\mu$ F
Low-side half-bridge capacitor $C_1 C_2$	100 $\mu$ F
High-side half-bridge capacitor $C_3 C_4$	30 $\mu$ F
MOSFET $S1 S2 S3 S4$	SCT2450KE
Diode $D_{S1} D_{S2} D_{S3} D_{S4}$	STTH10LCD06

▪ **Comparison between Si and SiC type SCT2450KE MOSFET**

Component	Si(STP8NK100Z)	SiC(SCT2450KE)
Rise Time $t_r$	3 ns	17 ns
Fall Time $t_f$	30 ns	34 ns
$R_{DS(on)}$	3.50 $\Omega$	0.45 $\Omega$
Switching loss	1.05 W	0.85 W
On-state loss	87.5 W	11.2 W



# **Appendix B**

## **(References)**

## **References**

- 1) *A Literature Survey on Bidirectional DC to DC Converter*, by Sasikumar S, Research Scholar, Department of Electrical Engineering , Sona College of Technology and Krishnamurthy K, Associate Professor, Department of Electrical Engineering ,Sona College of Technology; *Volume IV, Issue X, October 2015, IJLTEMAS, ISSN 2278 – 2540*
- 2) Krismer, F. *Modeling and Optimization of Bidirectional Dual Active Bridge DC DC Converter Topologies*. Ph.D. Thesis, ETH Zurich, Zurich, Switzerland, 2010.
- 3) Kheraluwala, M.N.; Gascoigne, R.W.; Divan, D.M.; Baumann, E.D. *Performance Characterization of a High-Power Dual Active Bridge dc-to-dc Converter*. IEEE Trans. Ind. Appl. 1992, 28, 1294–1301.
- 4) Bai, H.; Mi, C. *Eliminate reactive power and increase system efficiency of isolated bidirectional dual-active-bridge dc-dc converters using novel dual-phase-shift control*. IEEE Trans. Power Electron. 2008, 23, 2905–2914.
- 5) Zhao, B.; Song, Q.; Liu, W. *Power characterization of isolated bidirectional dual-active-bridge dc-dc converter with dual-phase-shift control*. IEEE Trans. Power Electron. 2012, 27, 4172–4176.
- 6) Krismer, F.; Kolar, J.W. *Efficiency-optimized high-current dual active bridge converter for automotive applications*. IEEE Trans. Ind. Electron. 2012, 59, 2745–2760.
- 7) Flores, L.A.; García, O.; Oliver, J.A.; Cobos, J.A. *High-frequency Bi-directional DC/DC converter using two inductor rectifier*. IECON Proc. (Ind. Electron. Conf.) 2006, 2793–2798.
- 8) De Doncker, R.W.; Divan, D.M.; Kheraluwala, M. *A three-phase soft-switched high power density dc/dc converter for high power applications*. IEEE Trans. Ind. Appl. 1991, 27, 63–73.
- 9) Bhat, A.K.S.; Member, S. *Fixed-Frequency PWM Series-Parallel Resonant Converter*. IEEE Trans. Ind. Appl. 1992, 28, 1002–1009.
- 10) Pan, X.; Li, H.; Liu, Y.; Tianyang, Z.; Ju, C.; Rathore GAE, A.K. *An Overview and Comprehensive Comparative Evaluation of Current-Fed Isolated Bidirectional DC/DC Converter*. IEEE Trans. Power Electron. 2019, 35, 2737–2763.
- 11) De, D.; Castellazzi, A.; Lamantia, A. *1.2 kW dual-active bridge converter using SiC power MOSFETs and planar magnetics*. In Proceedings of the 2014 International Power Electronics Conference, IPEC-Hiroshima—ECCE Asia 2014, Hiroshima, Japan, 18–21 May 2014; pp. 2503–2510.
- 12) R. Dhar and S. Mukherjee, “Design of APOD-PWM Based Multi-level Inverter using Cuk DC–DC Converter with MPPT,” in *Intelligent Electrical Systems: A Step towards Smarter Earth*, 1st Editio., A. K. B. Satyajit Chakrabarti, Ayan Kumar Panja, Amartya Mukherjee, Ed. Boca Raton: CRC Press, 2021, pp. 241–255.
- 13) S. Mukherjee, S. De, S. Sanyal, S. Das, and S. Saha, “A 15-level asymmetric H-bridge multilevel inverter using d-SPACE with PDPWM technique,” *Int. J. Eng. Sci. Technol.*, vol. 11, no. 1, pp. 22–32, 2019

- 14)** Buticchi, G.; Costa, L.; Liserre, M. *Improving System Efficiency for the More Electric Aircraft: A Look at  $dc_n/dc$  Converters for the Avionic Onboard  $dc$  Microgrid*. IEEE Ind. Electron. Mag. 2017, 11, 26–36.
- 15)** Buticchi, G.; Costa, L.F.; Barater, D.; Liserre, M.; Amarillo, E.D. *A Quadruple Active Bridge Converter for the Storage Integration on the More Electric Aircraft*. IEEE Trans. Power Electron. 2018, 33, 8174–8186.
- 16)** *A Survey on Bidirectional DC/DC Power Converter Topologies for the Future Hybrid and All Electric Aircrafts*, Álvaro Ojeda-Rodríguez, Pablo González-Vizueté, María A. Martín-Prats, Dpto. Ingeniería Electrónica, Escuela Técnica Superior de Ingeniería, Universidad de Sevilla, 41092 Seville, Spain; aorodriguez@us.es (Á.O.-R.); pgonzalez17@us.es (P.G.-V.); mmprats@us.es (M.A.M.-P.), Joaquín Bernal-Méndez, Dpto.Física Aplicada III, Escuela Técnica Superior de Ingeniería, Universidad de Sevilla, 41092 Seville, Spain. Received: 24 July 2020; Accepted: 7 September 2020; Published: 17 September 2020.
- 17)** Brandelero, J.C. *Conception et Réalisation d' un Convertisseur Multicellulaire DC/DC Isolé Pour Application Aéronautique*. Ph.D. Thesis, INP de Toulouse, Toulouse, France, 2015.
- 18)** Asfaux, P.; Bourdon, J. *Development of a 12 kW isolated and bidirectional DC-DC Converter dedicated to the More Electrical Aircraft: The Buck Boost Converter Unit (BBCU)*. In *Proceedings of the PCIM Europe 2016, International Exhibition and Conference for Power Electronics, Intelligent Motion, Renewable Energy and Energy Management, Nuremberg, Germany*, 10–12 May 2016; pp. 1814–1821.
- 19)** Tarisciotti, L.; Costabeber, A.; Chen, L.; Walker, A.; Galea, M. *Current-Fed Isolated DC/DC Converter for Future Aerospace Microgrids*. In *IEEE Transactions on Industry Applications; Institute of Electrical and Electronics Engineers Inc.*: Piscataway, NJ, USA, 2019; Volume 55, pp. 2823–2832.
- 20)** *DC-DC converter with 50 kHz-500 kHz range of switching frequency for passive component volume reduction*. Article in International Journal of Electrical and Computer Engineering · April 2021 DOI: 10.11591/ijece.v11i2.pp1114-1122; by Mohd Amirul Naim Kasiran, University Tun Hussein Onn Malaysia, Asmarashid Ponniran, Universiti Tun Hussein Onn Malaysia, Mohd Hafizie Yatim, Universiti Tun Hussein Onn Malaysia
- 21)** S. Mukherjee, S. S. Saha and S. Chowdhury, "Design of Duty-Ratio and Phase-Shift Control Circuits for MPPT of SPV Source using ZV-ZCS PSFB Converters," *2021 Devices for Integrated Circuit (DevIC)*, 2021, pp. 555-559, doi: 10.1109/DevIC50843.2021.9455893.
- 22)** *Soft-Switching Bidirectional DC/DC Converter with a LCLC Resonant Circuit*; Yijie Wang, Senior Member, IEEE, Hongyu Song, Dianguo Xu, Fellow, IEEE; IEEE Journal of emerging and selected Topics in Power Electronics, 2019
- 23)** Z. Zhang and P. Wang, *Research and Implementation of Natural Sampling SPWM Digital Method for three-level Inverter of Photovoltaic Power Generation System based on FPGA*; National Natural Science of Foundation of China, August 2019.
- 24)** K. Suresh and E. Parimalasundar, *A modified multi-level inverter with Inverted SPWM Control*; IEEE Canadian Journal of Electrical and Computer Engineering, Vol. 45, no. 2, pp. – 99-104, 2022
- 25)** J. Huang and R. Xiong, *Study on Modulating Carrier Frequency Twice in SPWM in SPWM Single phase inverter*; IEEE transactions on Power Electronics, vol. 29, no. 7, pp. – 3384-3392, July 2014

**24)** Behdad Faridpak, Meisam Farrokhifar, *Senior Member, IEEE*, Mojtaba Nasiri, Arman Alahyari, Nasser Sadoogi; *Developing a Super-lift LUO-Converter with Integration of Buck Converters for Electric Vehicle Applications*; CSEE Journal of Power and Energy Systems, August 2020.

**25)** *Power Electronics*, Second Edition; M.D. Singh, *Former Principle, Laxmi Narayan College of Technology, Bhopal* and K.B. Khanchandani, *Professor and Head, Department of Electronics and communication Engineering, SSGM College of Engineering, Shegaon, Maharashtra*